(12)

AFWAL-TR-80-4204

THREE-DIMENSIONAL NATURE OF STRAIN FIELD NEAR COLDWORKED HOLES·

Gary Cloud
Somnuek Paleebut

Division of Engineering Research
Michigan State University
East Lansing, MI 48824

May 1982

Final Report for Period June 1978 to February 1980

Approved for public release; distribution unlimited

MATERIALS LABORATORY
AIR FORCE WRIGHT AERONAUTICAL LABORATORIES
AIR FORCE SYSTEMS COMMAND
WRIGHT-PATTERSON AIR FORCE BASE, OHIO 45433

NOTICE

When Government drawings, specifications, or other data are used for any purpose other than in connection with a definitely related Government procurement operation, the United States Government thereby incurs no responsibility nor any obligation whatsoever; and the fact that the government may have formulated, furnished, or in any way supplied the said drawings, specifications, or other data, is not to be regarded by implication or otherwise as in any manner licensing the holder or any other person or corporation, or conveying any rights or permission to manufacture use, or sell any patented invention that may in any way be related thereto.

This report has been reviewed by the Office of Public Affairs (ASD/PA) and is releasable to the National Technical Information Service (NTIS). At NTIS, it will be available to the general public, including foreign nations.

This technical report has been reviewed and is approved for publication.

Robert C. Donath

ROBERT C. DONATH
Project Engineer

John P. Henderson

JOHN P. HENDERSON
Metals Behavior Branch
Metals and Ceramics Division

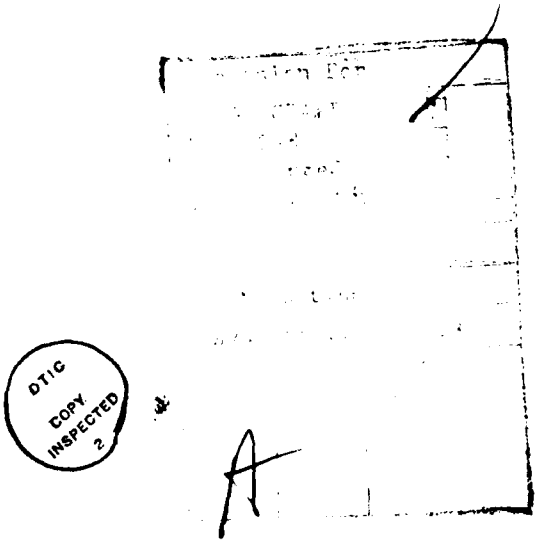

"If your address has changed, if you wish to be removed from our mailing list, or if the addressee is no longer employed by your organization please notify AFWAL/MLLN, *W-PAFB, OH 45433 to help us maintain a current mailing list".*

Copies of this report should not be returned unless return is required by security considerations, contractual obligations, or notice on a specific document.

AIR FORCE/56780/24 June 1982 — 350

UNCLASSIFIED

SECURITY CLASSIFICATION OF THIS PAGE (When Data Entered)

REPORT DOCUMENTATION PAGE

READ INSTRUCTIONS BEFORE COMPLETING FORM

1. REPORT NUMBER: AFWAL-TR-80-4204	2. GOVT ACCESSION NO. A0113424
3. RECIPIENT'S CATALOG NUMBER	
4. TITLE (and Subtitle): THREE-DIMENSIONAL NATURE OF STRAIN FIFLD NEAR COLDWORKED HOLES	5. TYPE OF REPORT & PERIOD COVERED: Final Report for period June 1978 - February 1980
	6. PERFORMING ORG. REPORT NUMBER
7. AUTHOR(s): Gary Cloud and Somnuek Paleebut	8. CONTRACT OR GRANT NUMBER(s): F33615-78-C-5123
9. PERFORMING ORGANIZATION NAME AND ADDRESS: Division of Engineering Research, Michigan State University, East Lansing, MI 48824	10. PROGRAM ELEMENT, PROJECT, TASK AREA & WORK UNIT NUMBERS: 2418 03 03
11. CONTROLLING OFFICE NAME AND ADDRESS: Materials Laboratory, Air Force Wright Aeronautical Labs, Wright-Patterson AFB, Ohio 45433	12. REPORT DATE: May 1982
	13. NUMBER OF PAGES
14. MONITORING AGENCY NAME & ADDRESS (if different from Controlling Office)	15. SECURITY CLASS. (of this report): UNCLASSIFIED
	15a. DECLASSIFICATION/DOWNGRADING SCHEDULE

16. DISTRIBUTION STATEMENT (of this Report)

Approved for public release; distribution unlimited.

17. DISTRIBUTION STATEMENT (of the abstract entered in Block 20, if different from Report)

18. SUPPLEMENTARY NOTES

19. KEY WORDS (Continue on reverse side if necessary and identify by block number)

Fasteners	Plasticity
Holes	Strain
Coldwork	Moire

20. ABSTRACT (Continue on reverse side if necessary and identify by block number)

As part of a comprehensive program to develop understanding of fatigue-rated fasteners, the three-dimensional aspects of the radial, hoop, and transverse strains which are created by drawing a tapered mandrel through a cylindrical hole were measured. A unique 3-dimensional moiré procedure was used. Specimens were fabricated with multiple embedded grids. These grids were photographed for each specimen state. Moiré fringe photographs were extracted from the replicas by coherent optical processing. Digital analysis of the fringes

DD FORM 1 JAN 73 1473 EDITION OF 1 NOV 65 IS OBSOLETE

UNCLASSIFIED

SECURITY CLASSIFICATION OF THIS PAGE (When Data Entered)

gave the desired strain maps. The residual radial strain after coldwork inside the specimen was found to be smaller than on the surface. The transverse strain changes from tension near the top surface where the mandrel enters to maximum compression at the midplane, where it begins to decrease. The hoop strain is maximum on the entry surface and decreases to a minimum at the midplane. The change in this component is only about four percent of the maximum value. Potential problems in the use of such coldworking processes might arise from the low value of the interior radial strain in comparison with the surface value and the existence of tensile transverse normal strain near the surface.

FOREWORD

This report was prepared by the Department of Metallurgy, Mechanics and Materials Science, Michigan State University, East Lansing, Michigan 48824, under Contract No. F33615-78-C-5123, "Coldworked Hole Stress Analysis." The contract, which was initiated under Project No. 2418, Task 24180305, was administered under the direction of the Air Force Materials Laboratory, Metals Behavior Branch (AFWAL/MLLN), by Dr. Robert C. Donath, Project Engineer.

The research reported herein was submitted by Dr. Gary Cloud who was the Principal Investigator, and covers work conducted during the period June 1978 to February 1980.

TABLE OF CONTENTS

LIST OF ILLUSTRATIONS

LIST OF ILLUSTRATIONS (CONTINUED)

LIST OF ILLUSTRATIONS (CONTINUED)

SUMMARY

The experimental results in this investigation are restricted to the strain maps along the thickness near the edge of the hole while the specimen is being coldworked and after coldwork is completed. The strain was measured by a moiré technique which gave information about the radial, hoop, and transverse normal strain fields near the edge of the hole as a function of distance from the specimen surface.

The moiré fringe pattern near the edge of the hole along the thickness changed when the tapered mandrel was pulled down. The diametral expansion was found not to be uniform along the thickness. The expansion inside the specimen was smaller than on the surface.

While the specimen was being coldworked, the strain was different along the thickness depending on the thickness of each specimen, and the shape of the mandrel. The strains were not uniform along the specimen thickness, and the measured strains on both sides were not quite the same. The strain in the radial direction inside the specimen was smaller than on the surface after the specimen was coldworked. The maximum strain occurred near the edge of the hole and decreased with increasing distance from the hole. The strain in the z-direction was tension near the top surface and changed to compression along the thickness; the maximum occurred near the midplane, and the strain decreased towards the bottom. After passing through a minimum, the transverse strain increased in compression again near the bottom. The hoop strain was a maximum on the top surface, decreased to a minimum at the midplane and appeared to increase towards the bottom surface.

The fact that the radial normal strain in the interior of the specimen on the hole boundary is small when compared with the surface strain is troubling from the viewpoint of fatigue design with coldwork-type fasteners.

The creation of tensile transverse normal strain near the surface, however, is potentially more of a problem. It is recognized, though, that the transverse stress would be modified by installation of a fastener, such as a bolt, which induces compression in the material.

SECTION I

INTRODUCTION

Because they create areas of high stress and increase the number of potential crack-initiation sites, holes often shorten the operational life of structural components. It is important to develop better understanding of crack initiation and growth from holes and also to devise techniques for decreasing the probability for failure to begin at holes.

One approach to improving the fatigue performance of a component containing a hole is to plastically expand the hole. Design procedures for such expanded or coldworked holes are still in the early stages of development. Progress has been impeded by lack of knowledge of the stress and strain fields induced by plastic radial expansion. Pioneering efforts by several investigators to obtain needed data and to develop design approaches have been described by Cloud (1,2), and there is little need to review them again here.

A program designed to develop an understanding of the behavior of coldworked holes in the presence of plate edges, compressive loads and adjacent fasteners has been described in detailed reports by Cloud and Tipton (3) and by Cloud and Sulaimana (4). A part of that program included experiments to investigate the three-dimensional aspects of the strain field near plastically enlarged holes. These experiments and the results are described herein. It is useful to keep in mind, as this work is reviewed, that this report is part of a program which produced two earlier reports (3,4), and that all of these reports are related to one another.

The three-dimensional nature of the radial, hoop, and transverse strains created by mandrelizing were explored in order to establish whether the

interior values of strain correlate well with surface values as established by measurement or calculation.

Experimental three-dimensional strain fields can be studied by only a few methods. The embedded grid moiré technique (5, for example) seemed most appropriate for this problem. Such approaches have been limited, however, by the necessity of using only one embedded grid or grating. During the course of this and related work,* the investigators discovered that several interior gratings could be used and that each grating can be individually observed and photographed even though other gratings might tend to obstruct the view. Such a procedure yields individual grating replicas for each interior and surface plane for each state of the specimen. These grating photographs can then be processed to obtain moiré fringe patterns, and those fringe patterns analyzed to obtain strain maps, using the optical and computer procedures described by Cloud (1-4).

SECTION II

SPECIMEN FABRICATION AND MATERIALS SPECIFICATION

The materials used for this investigation included polycarbonate resin and a mixture of flexible and rigid polyester resins. In the beginning polycarbonate resin was used. A polycarbonate sheet obtained from the Mobay Chemical Company was cut into two rectangular pieces and a copper grating was printed on one of the surfaces. The blocks were then glued together to form a specimen block with the copper grating at the midplane.

---

* This unique moiré method using multiple-embedded gratings for investigating 3-dimensional strain fields was developed by the Principal Investigator under National Science Foundation Grant ENG-7802530. It has not yet been described in the technical literature. Details will be provided by the Principal Investigator when requested.

Poisson's ration of polycarbonate is 0.45. The modulus of elasticity as a function of temperature, and a typical stress-strain curve are shown in Figure 1 and Figure 2, respectively. These data are from an Engineering Handbook on Merlon Polycarbonate by the Mobay Chemical Company, Pittsburgh, Pennsylvania (6).

A mixture of flexible and rigid polyester resins was used to make the other specimens. D. H. Morris and W. F. Riley (7) show that a mixture of 60% by weight flexible MR-9600 (previously designated EPX-126-3) and 40% by weight Laminac 4116 can be used to predict the behavior of an aluminum prototype. The Poisson's ratio was found by them to be 0.45. Their stress-strain curves, which depend on strain rate, are reproduced in Figure 3.

These particular resins are now marketed by the USS Chemicals Division of United States Steel, Polyester Unit. The 60:40 mixture by weight was used. The two resins were first blended with 1% methyl-ethyl-peroxide cast in an aluminum mold. Nickle mesh with 500 lines per inch (20 lines per mm) and 0.0008 inches (0.0203 mm) thickness (marketed by the Buckbee Mears Company) was retained at the center of the mold and the resin poured around it. The resin was allowed to cure at room temperature for 24 hours. The partially set specimen was then removed from the mold, left in an oven, and post-cured at 80° C for 16 hours.

The dimensions of all the specimens used for this investigation are shown in Figure 4-a. The hole with a diameter of 0.25 inches (6.35 mm) was drilled and reamed at the center of the specimen for the coldworking process. The fiducial marks were made by drilling a small hole 1/32 inches (0.794 mm) in diameter on the grating line at a distance of 0.5 inches (12.7 mm) from the center of the large hole as shown in Figure 4-b. All specimens were polished to get a smooth and clear surface to let the light pass through without scattering or deviation.

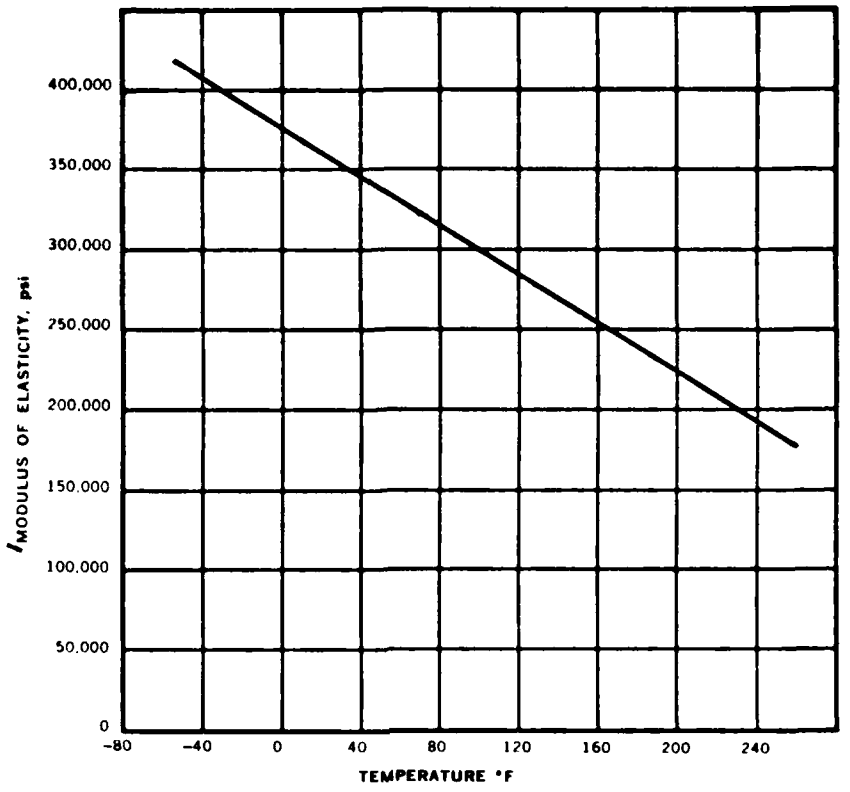

Figure 1. Modulus of Elasticity versus Temperature.

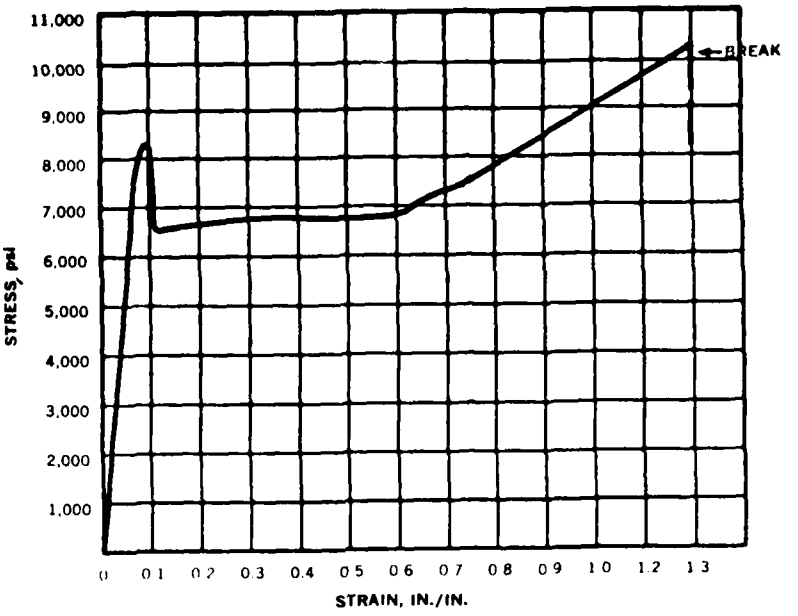

Figure 2. Stress-Strain Curve of Polycarbonate.

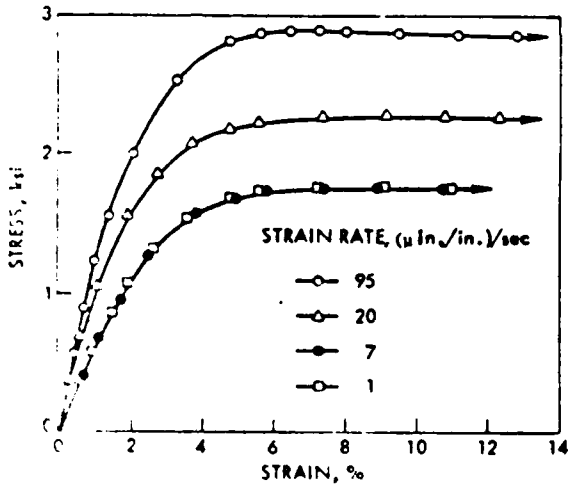

Figure 3. Stress-Strain Curves as a Function of Strain Rate for a 60:40 Mixture of Laminac Polyester Resins (Ref. 5).

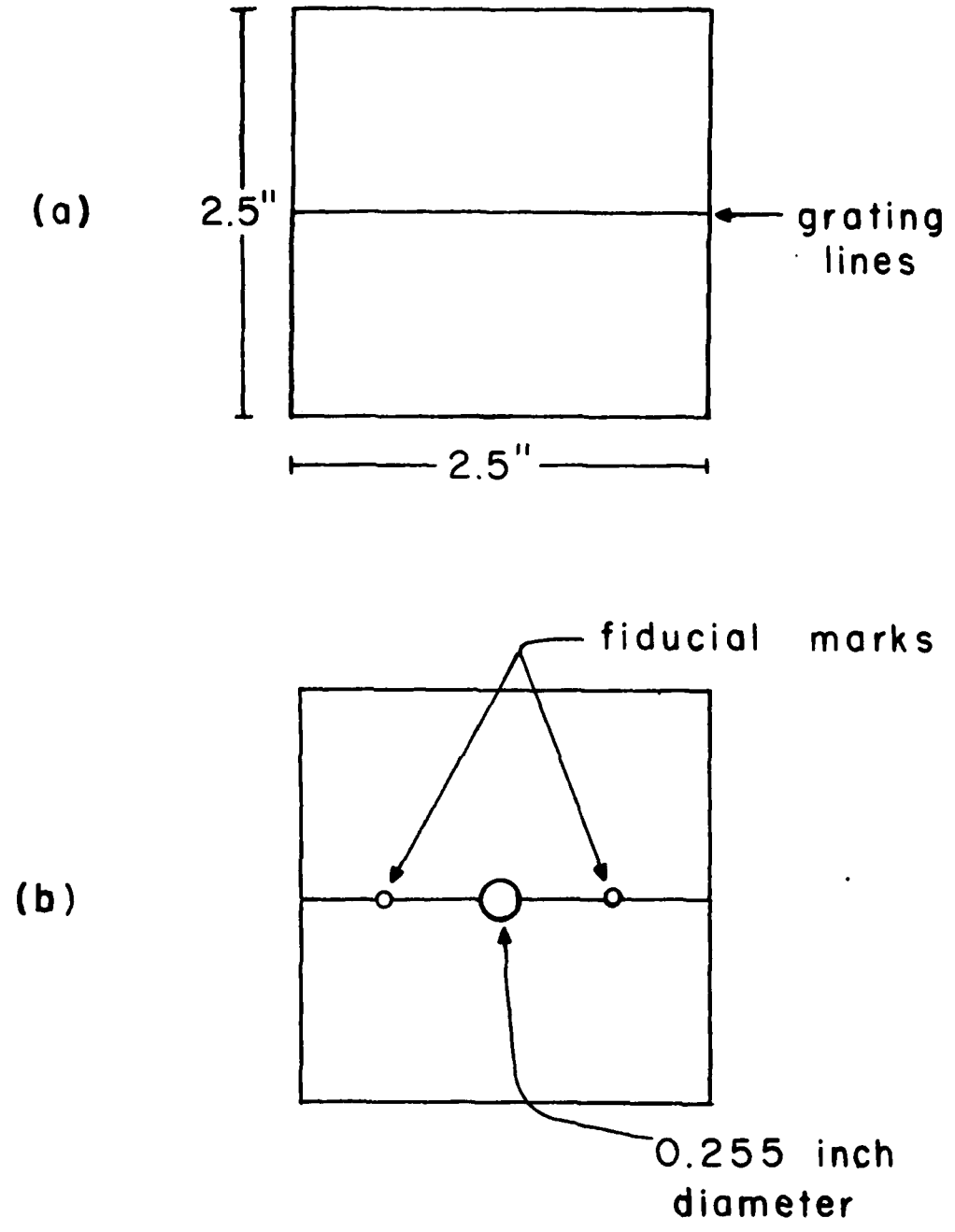

Figure 4. Specimen Dimensions.

SECTION III

GRID DEPOSITION

It was found that the photoresist could not be used to make a grating on the specimen surface because the grid would be destroyed when the other piece was glued over it. Therefore, specimens with copper gratings inside were used and gave fairly good results. In this study two methods, both described in published literature (8,9,10), were used to make a copper grating.

With the etching method, after the specimen was cleaned, a thin film of copper was deposited on the area of interest by using a Denton D.V.-502 High Vacuum Evaporator. The specimen was then sprayed with photoresist to cover the thin copper film. The two-way grating was printed by using a submaster grating having 1000 lines per inch (40 lines per mm), and finally the copper was etched with P. C. Board Etching Solution diluted with water 1:3 brushed one way. The specimen was then washed by water. This grating application process is summarized in Figure 5.

The stencil method used a fine metal mesh with an orthogonal array of holes. In this study nickel mesh with 500 lines per inch (20 lines per mm) was used. First, a nickel mesh was held in close contact with a specimen by spreading soap solution over it and then removing the surplus with filter paper. This removed the solution from the holes but left the mesh secured by a thin liquid layer under the lines. The specimen and mesh were placed in a vacuum unit, and copper was deposited through the holes of the mesh. Finally, the nickel mesh was removed from the specimen.

SECTION IV

COLDWORKING

The coldworking procedure used was developed by J. O. King, Inc.,

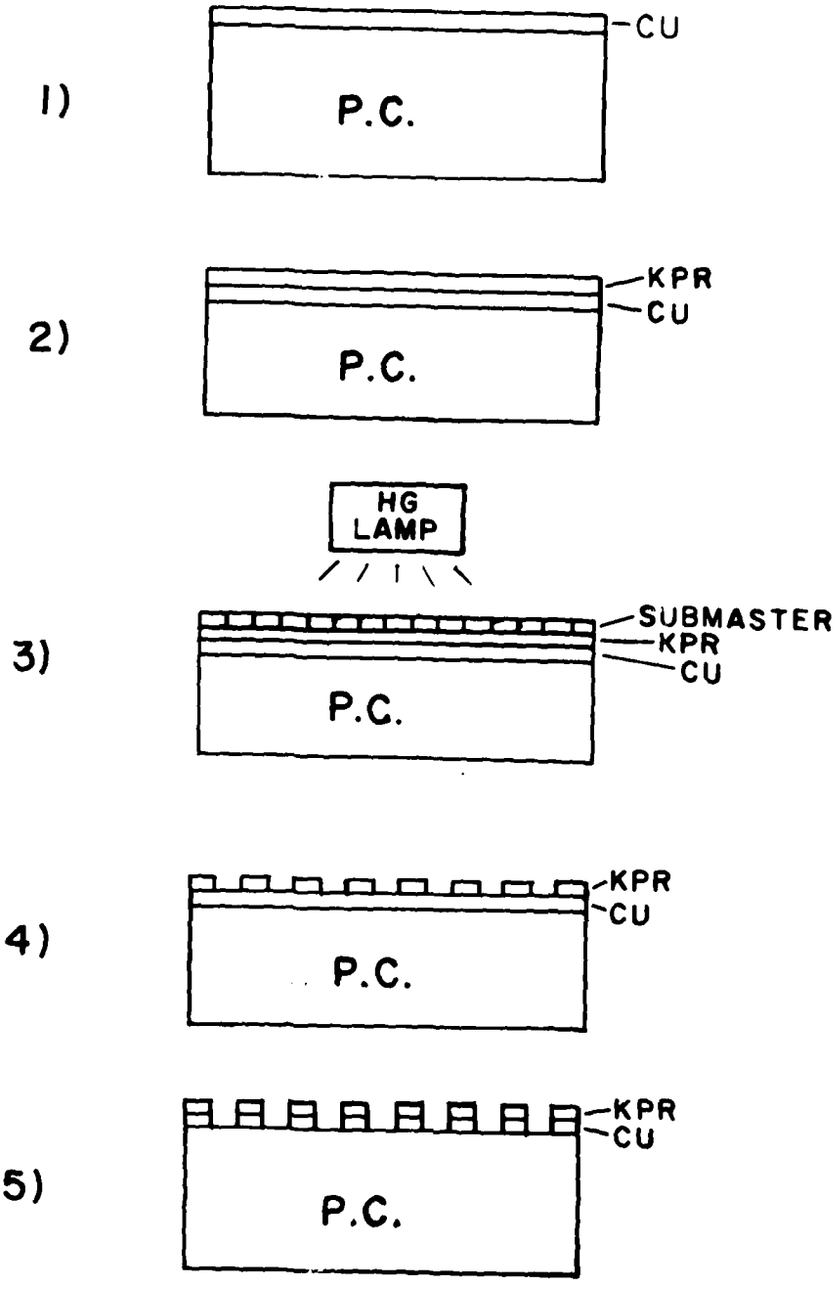

Figure 5. Copper Grating Etching Process.

711 Trabert Avenue, N. W., Atlanta, Georgia, 30318, and is described in the following paragraphs.

A thin-walled sleeve which carries an anvil on one end is inserted into the hole. A tapered mandrel is pulled through the hole to expand it while the anvil of the sleeve is supported to oppose the pulling force (see Figure 6). The mandrel enlarges the sleeve and expands the hole enough to cause plastic deformation around the hole. The sleeve remains in the hole but the anvil drops off. A machine incorporating a hand-operated hydraulic cylinder was constructed to pull the mandrel in the laboratory. The tapered mandrel used for this study had a maximum diameter of 0.2550 inches (6.4770 mm), the sleeve had a 0.2350 inch (5.9690 mm) inside diameter, a 0.2540 inch (6.4516 mm) outside diameter and was 0.0095 inches (0.2413 mm) in wall thickness.

The mandrelizing and testing sequence was accomplished in steps as follows:

1-a The tapered mandrel was pulled down until the top of the mandrel was at the same level as the top surface of the specimen.

1-b A grating photograph was recorded.

2-a The tapered mandrel was pulled down about 1/3 of the thickness.

2-b A grating photograph was recorded.

3-a The tapered mandrel was pulled down about 2/3 of the thickness.

3-b A grating photograph was recorded.

4-a The tapered mandrel was pulled out.

4-b A grating photograph was recorded.

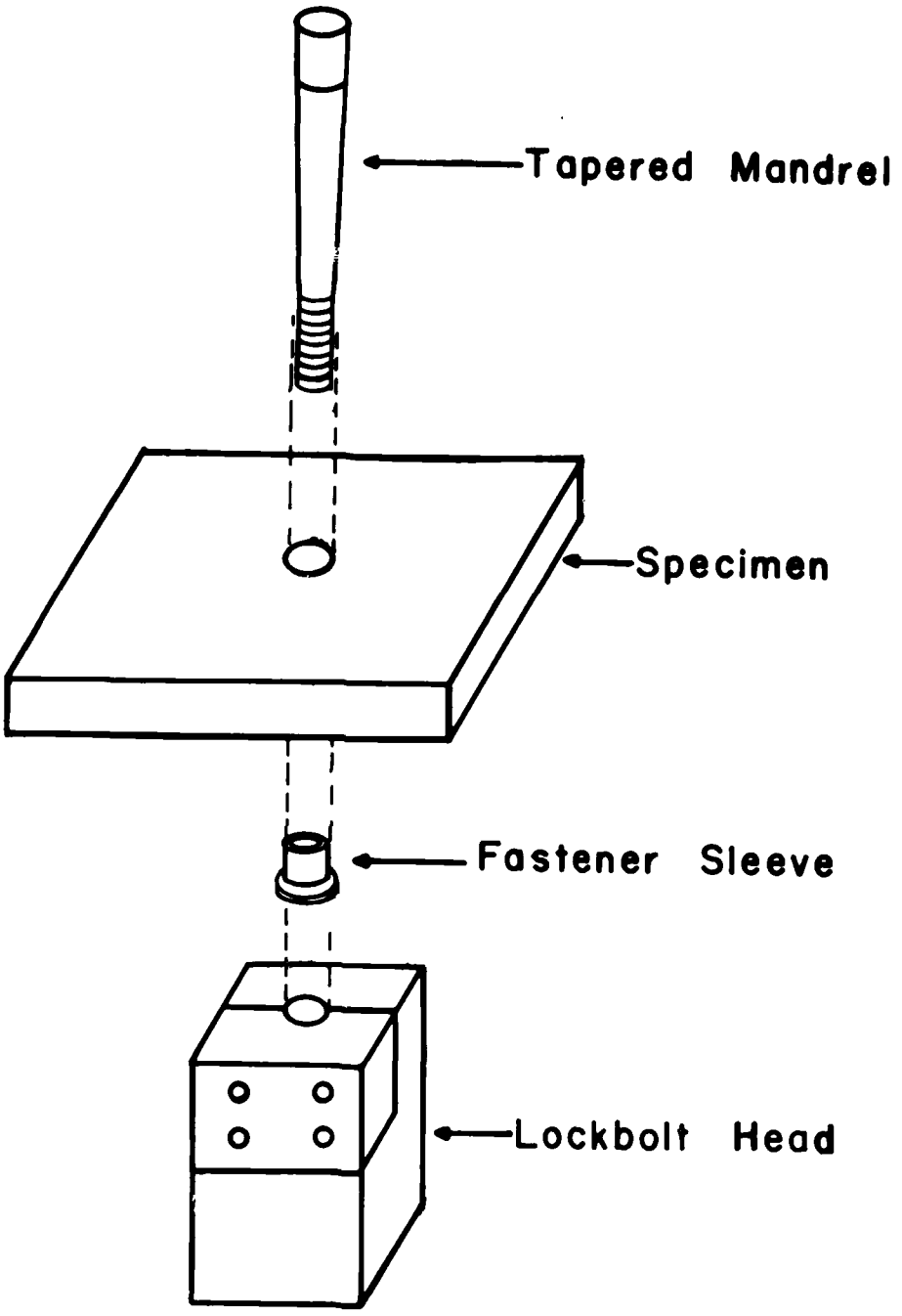

Figure 6. Schematic of the Coldworking Process.

SECTION V

PHOTOGRAPH OF SPECIMEN GRATING

The specimen was polished to get smooth, clear, and parallel surfaces which let light pass through it without scattering or causing optical distortion of the embedded grating. The system devised for photographing the specimen grating is shown schematically in Figure 7.

The camera used was a Tech/ops 4x5 bellows module. The lens was a Schnieder Krueznach, Retinar-Xenar with a focal length of 50 mm and a maximum aperture of 2.8. The system rested upon a granite optical table, and the camera was set up to give a magnification factor of 4. The specimen was placed on a specially designed holder. The light source for this work was a 150 W. General Electric Reflector Flood.

The image of the specimen grating in the emulsion of a test photoplate was examined with a Bausch and Lomb Optical Co. 10x magnifier, which had been adjusted to focus in the emulsion plane. The image of the specimen grating could be checked over the entire area near the edge of the hole along the thickness of the specimen for maximum sharpness and contrast. Kodak High Speed Holographic Film (SO-253, 4x5 in.) was used to take test photographs of the specimen grating. After getting the best grating from Kodak film, the data plates were made by using Kodak HIgh Speed Holographic Plates (Type 131-02, 4x5 in.). Five data plates were made for each specimen loading.

1. The specimen with no load; this data plate was used as a base line to eliminate error which might be induced by deformations created during fabrication of the specimen as well as various optical distortions.
2. The specimen with the top of the mandrel at the same level as the top surface of the specimen.

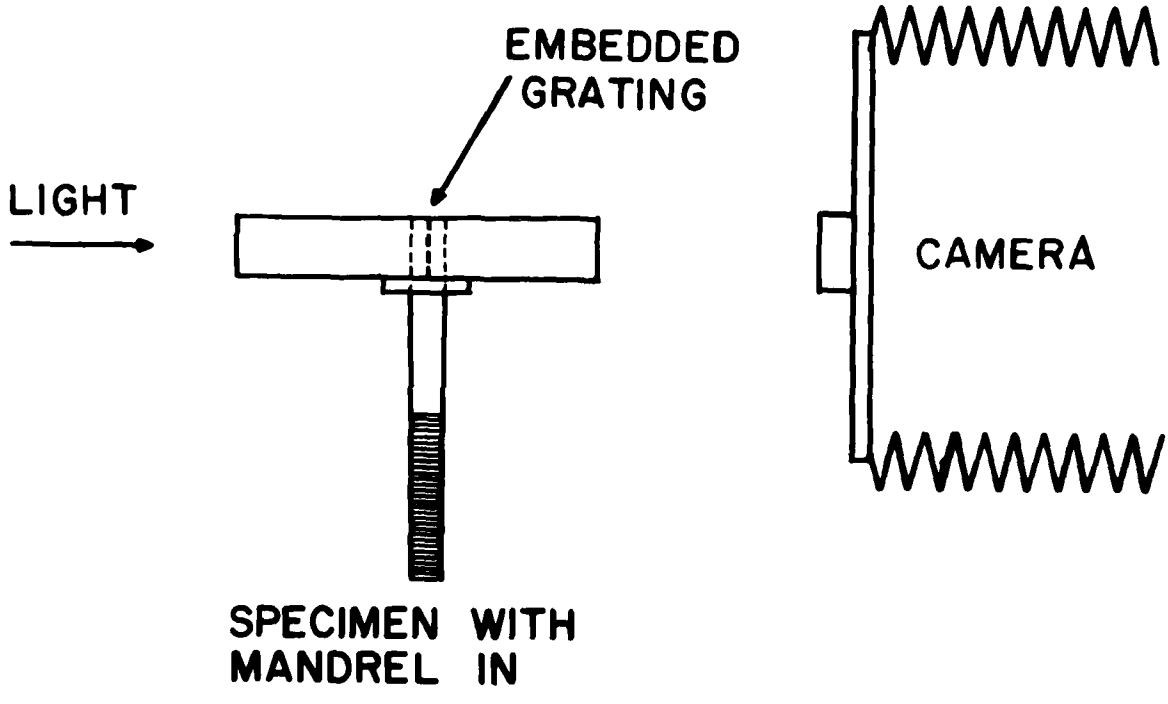

Figure 7. Schematic of the Photography Process.

3. The specimen with the top of the mandrel at 0.13 inches (3.302 mm) from the top surface of the specimen.
4. The specimen with the top of the mandrel at 0.24 inches (6.096 mm) from the top surface of the specimen.
5. The specimen without the mandrel (the mandrel was pulled out).

SECTION VI

SUMMARY OF OPTICAL PROCESSING

The grating photography stages of this experiment produced an assembly of photographic plates of the undeformed (baseline) and deformed (data) specimen gratings as well as several submaster gratings having various spatial frequencies. The creation of moiré fringe patterns and the reduction of moiré fringe data have been described in detail (1-4). The steps required to produce moiré fringe photographs from these grating records were as follows:

1. A photoplate of the undeformed grid was superimposed with a submaster grating having a spatial frequency of 3 (sometimes 2) times the frequency of the magnified specimen grating plus or minus a small frequency mismatch.
2. The superimposed gratings were clamped together and placed in a coherent optical processor and adjusted to produce a correct baseline (zero strain) fringe pattern at the processor output, where it was photographed.
3. Steps 1 and 2 were repeated with the photographs of the deformed grating in order to create the "data" or "at strain" fringe patterns.

4. The fringe patterns were enlarged and printed in a size equivalent to about 8 times the actual specimen dimensions with medium contrast.
5. The prints were sorted and coded for identification.
6. Computer digitizing, data reduction, and plotting were performed on each photograph.

SECTION VII

EXPERIMENTAL RESULTS AND DISCUSSION

The nature of the coldworking operation is to exert a force perpendicular to the specimen surface through the sleeve and thus create deformation of the hole. The diameter of the hole along the thickness was measured from the "unloaded" data plate and the "loaded" data plate (mandrel was passed through). Table 1 summarizes these results. Plots of the diameter of the hole before and after the load and the diametral expansions along the thickness of the specimen are shown in Figures 8 and 9, respectively. The deformation result shows that the hole is not uniformly expanded through the specimen by cold-work, and that the specimen has a minimum diametral expansion near its center.

TABLE 1. DIAMETER OF HOLE BEFORE AND AFTER LOAD

Distance from the top (in.)	Dia. of unloaded specimen (in.)	Dia. of loaded specimen (in.)	Diametral expansion (in.)
0.000	0.2574	0.2708	0.0134
0.130	0.2563	0.2695	0.0132
0.240	0.2551	0.2679	0.0128
0.381	0.2564	0.2713	0.0149
Average	0.2563	0.2700	0.0137

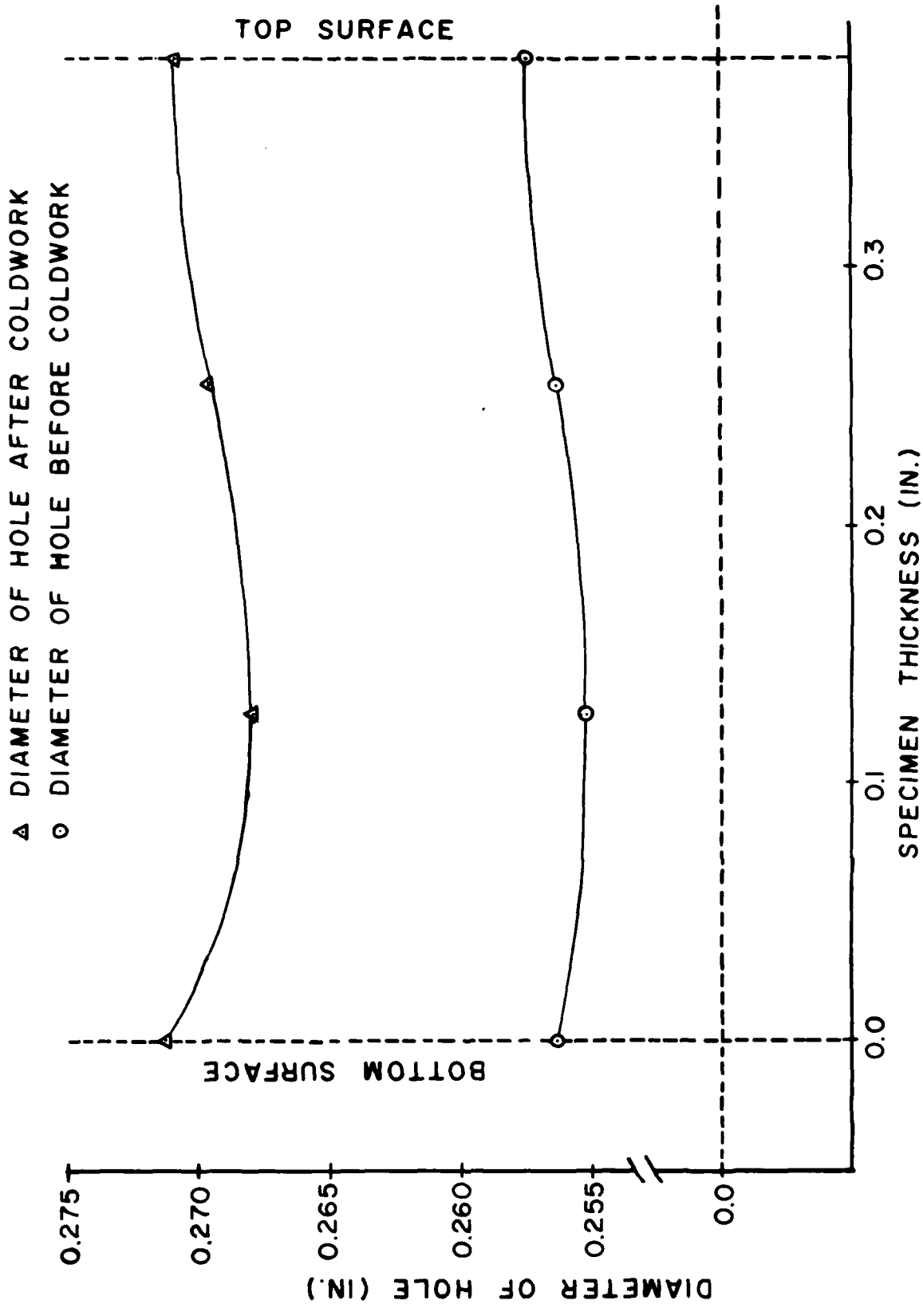

Figure 8. Diameter of the Hole Along the Thickness.

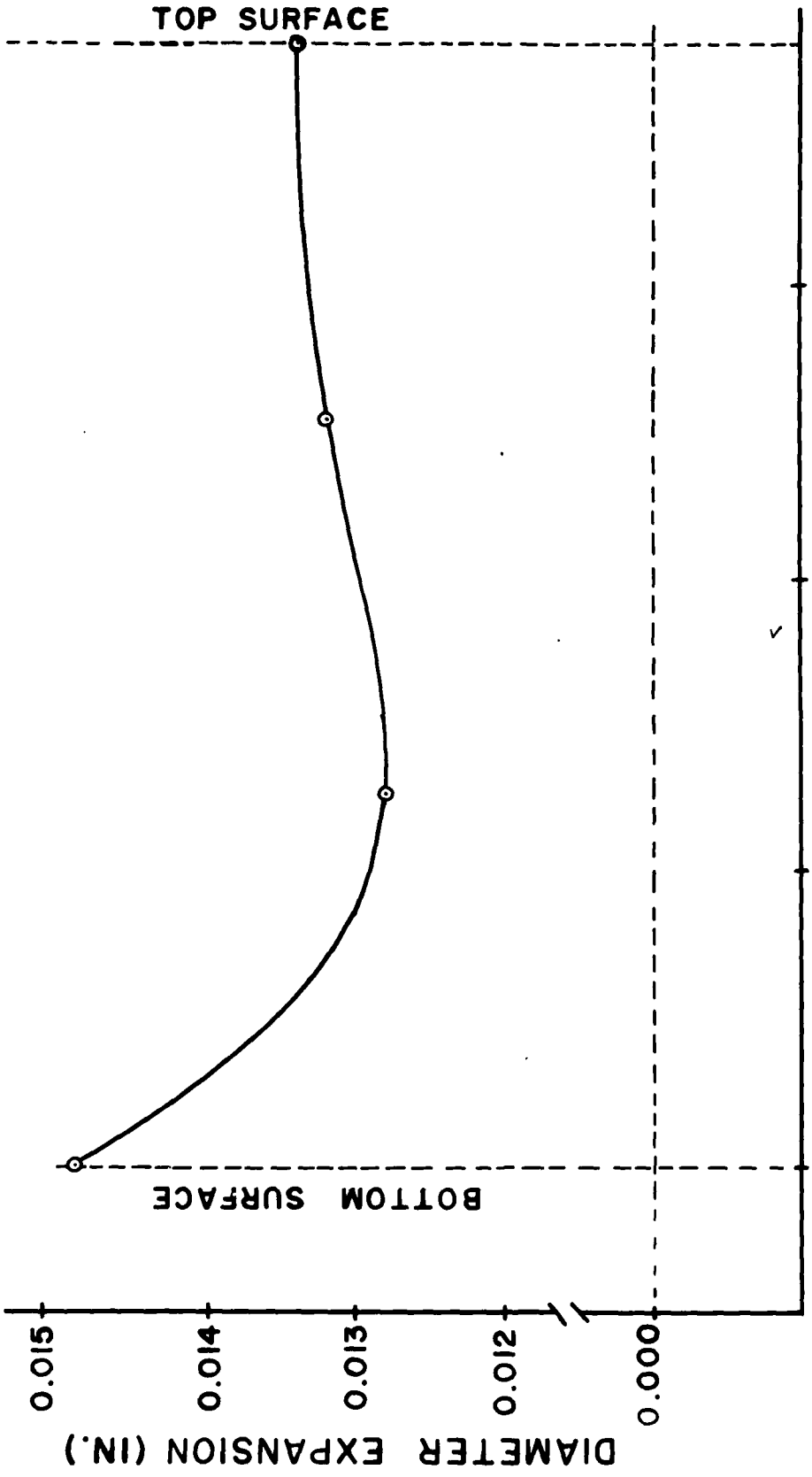

Figure 9. Diametral Expansions Along the Thickness.

In this investigation the specimen has a two-way grating (that is, an array of dots). By using the otpical processor, a moiré fringe pattern was formed separately for each direction. One pattern was formed to get vertical fringes (the direction parallel to the hole), and this fringe pattern was used to measure strain the the radial direction (the direction perpendicular to the hole). The other pattern was formed with horizontal fringes (the direction perpendicular to the hole); fringes in this direction were used to measure strain in the z-direction (the direction parallel to the hole). The photograph of the fringe pattern was recorded separately for each direction and for each loading step.

Photographs of the moiré fringe pattern obtained from the polycarbonate specimen for the vertical and horizontal directions are shown in Figures 10 to 14 and Figures 15 to 16, respectively. Because the polycarbonate specimen was found to be locally split along the grating plane after coldwork, the moiré fringe patterns were not entirely valid for the region near the hole. Because of the splitting that occurred, the analysis of the fringe data from the polycarbonate specimen was not completed.

The photographs of vertically-oriented (from the vertical grating) fringe patterns at each loading step obtained from the mixed polyester specimen are shown in Figures 17 to 21. The strain on the left and right sides at each loading step are shown in Figures 22 to 25 and Figures 26 to 29, respectively. At the first step, the top of the mandrel was pulled down to the level of the top surface of the specimen. The maximum expansion occurred at the top of the specimen, as shown in Figure 18, because the shape of the mandrel is a taper. The strain in the radial direction was measured to within 0.01 inches (0.254 mm) of the edge of the hole. The results show that the largest strain occurred within 0.1 inches (2.54 mm) of the edge of the hole

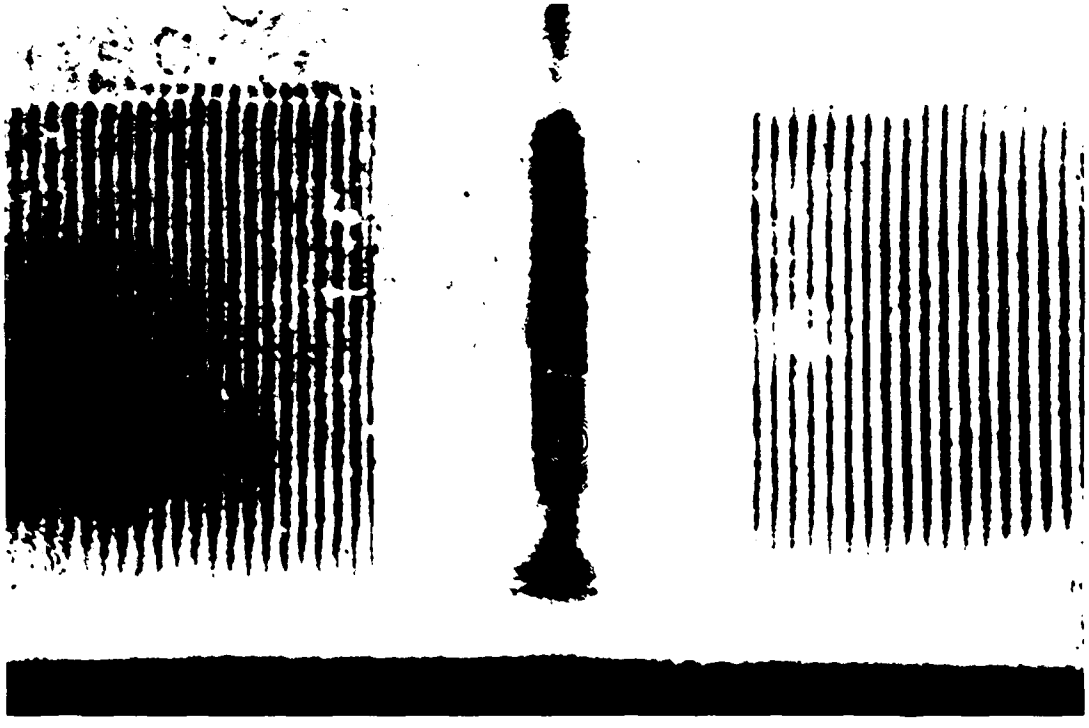

Figure 10. Photograph of Moiré Fringe Pattern with No-Load on Polycarbonate Test Specimen.

Figure 11. Photograph of Moiré Fringe Pattern with 1st-Step Load on Polycarbonate Test Specimen.

Figure 12. Photograph of Moiré Fringe Pattern with 2nd-Step Load on Polycarbonate Test Specimen.

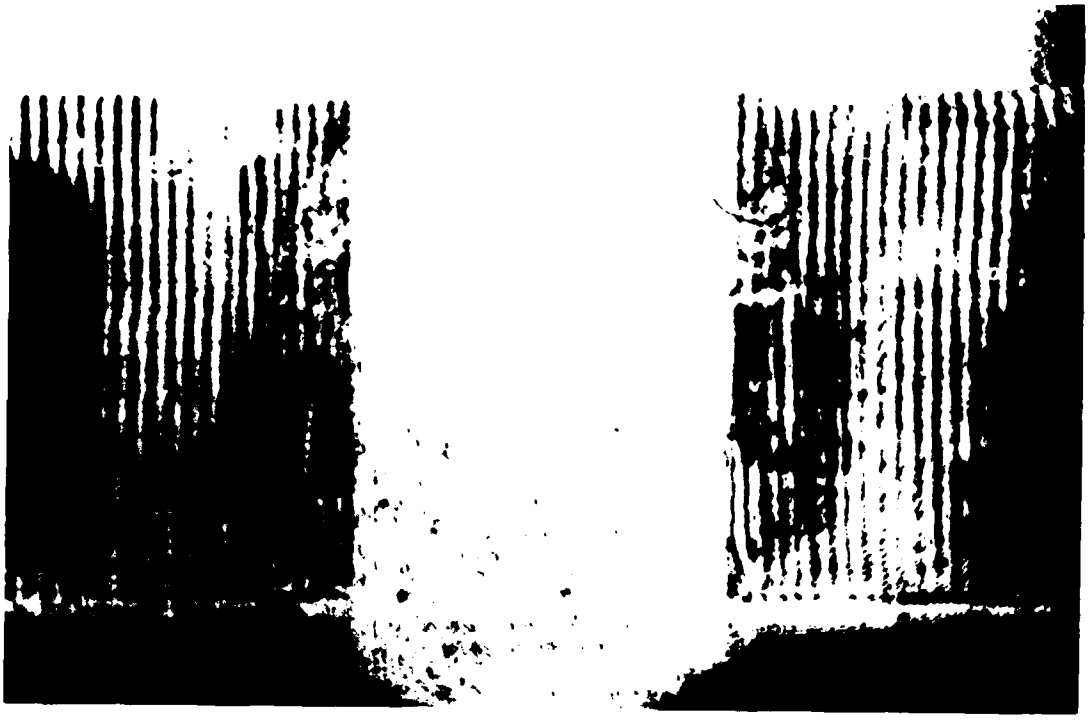

Figure 13. Photograph of Moiré Fringe Pattern with 3rd-Step Load on Polycarbonate Test Specimen.

Figure 14. Photograph of Moiré Fringe Pattern with 4th-Step Load on Polycarbonate Test Specimen.

Figure 15. Photograph of Moiré Fringe Pattern with No-Load of Polycarbonate Test Specimen.

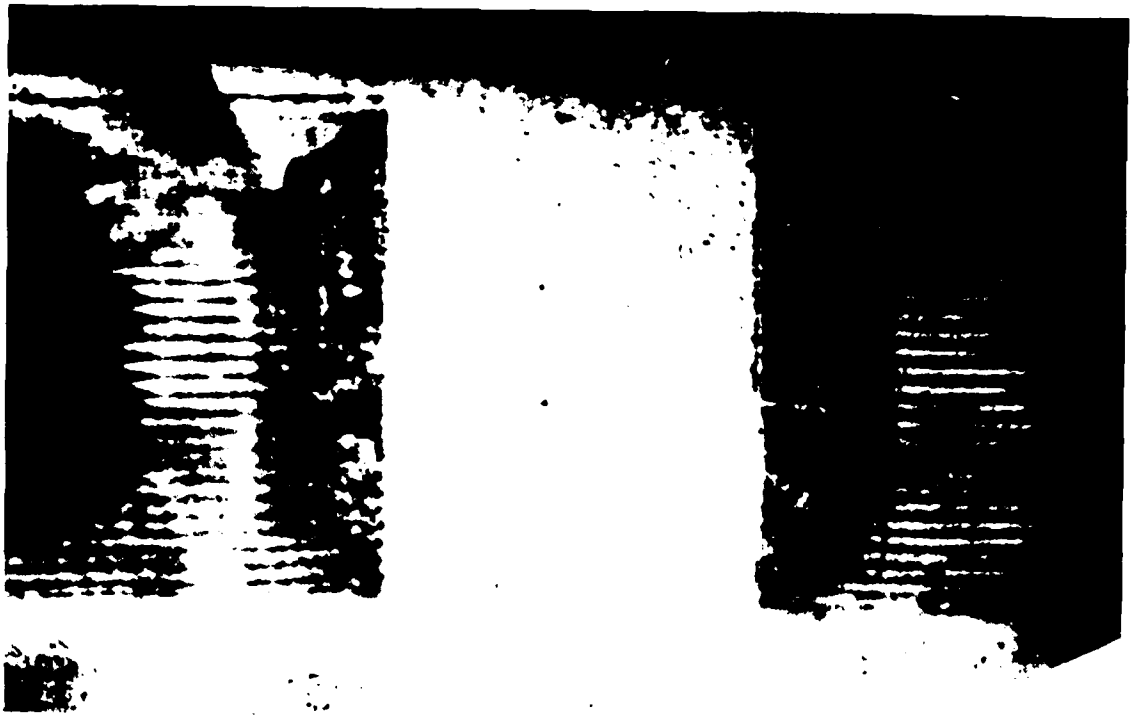

Figure 16. Photograph of Moiré Fringe Pattern after Coldworking of Polycarbonate Test Specimen.

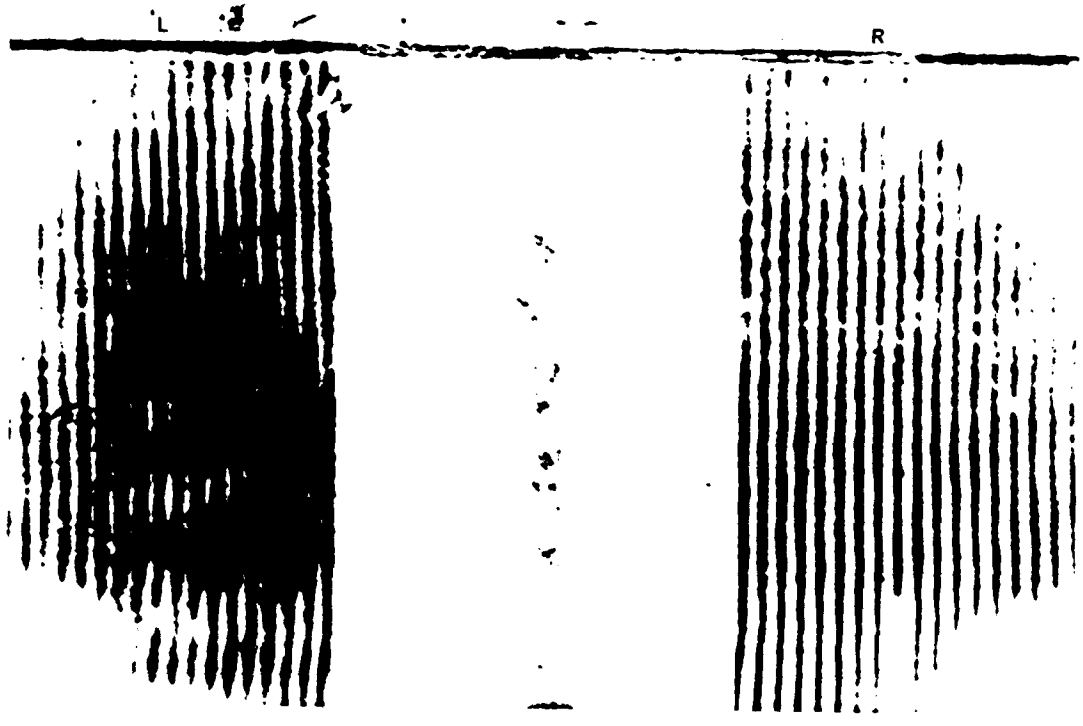

Figure 17. Photograph of Moiré Fringe Pattern with No-Load on Test Specimen of Mixed Polyester 60:40.

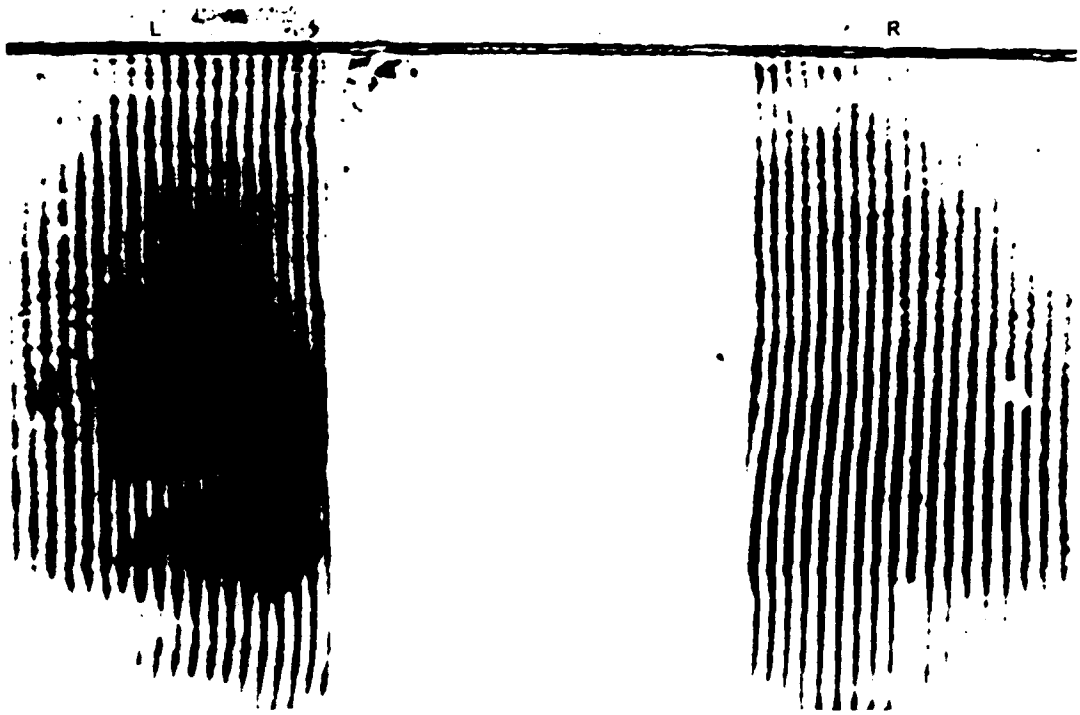

Figure 18. Photograph of Moiré Fringe Pattern with 1st-Step Load on Test Specimen of Mixed Polyester 60:40.

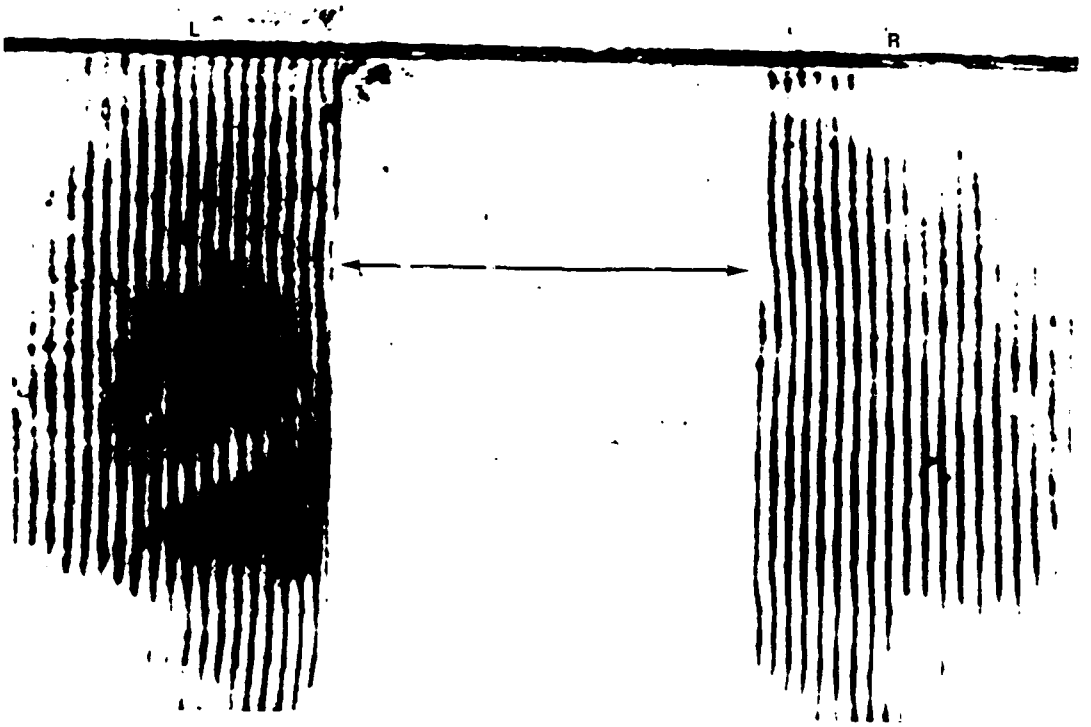

Figure 19. Photograph of Moiré Fringe Pattern with 2nd-Step Load on Test Specimen of Mixed Polyester 60:40.

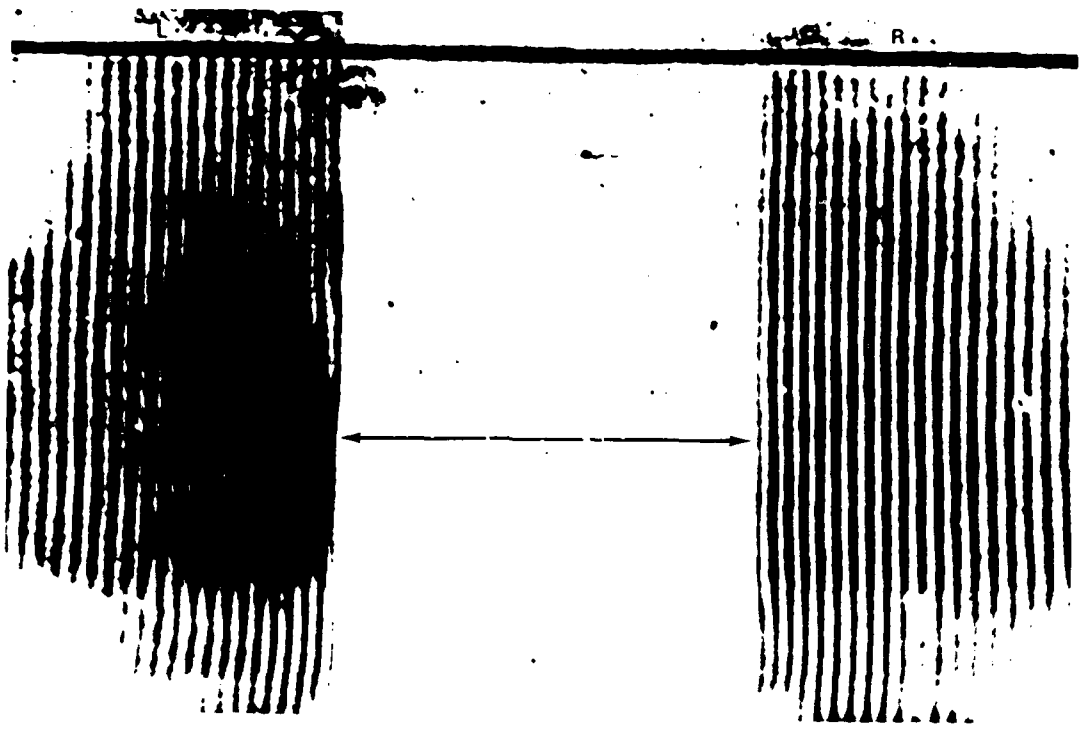

Figure 20. Photograph of Moiré Fringe Pattern with 3rd-Step Load on Test Specimen of Mixed Polyester 60:40.

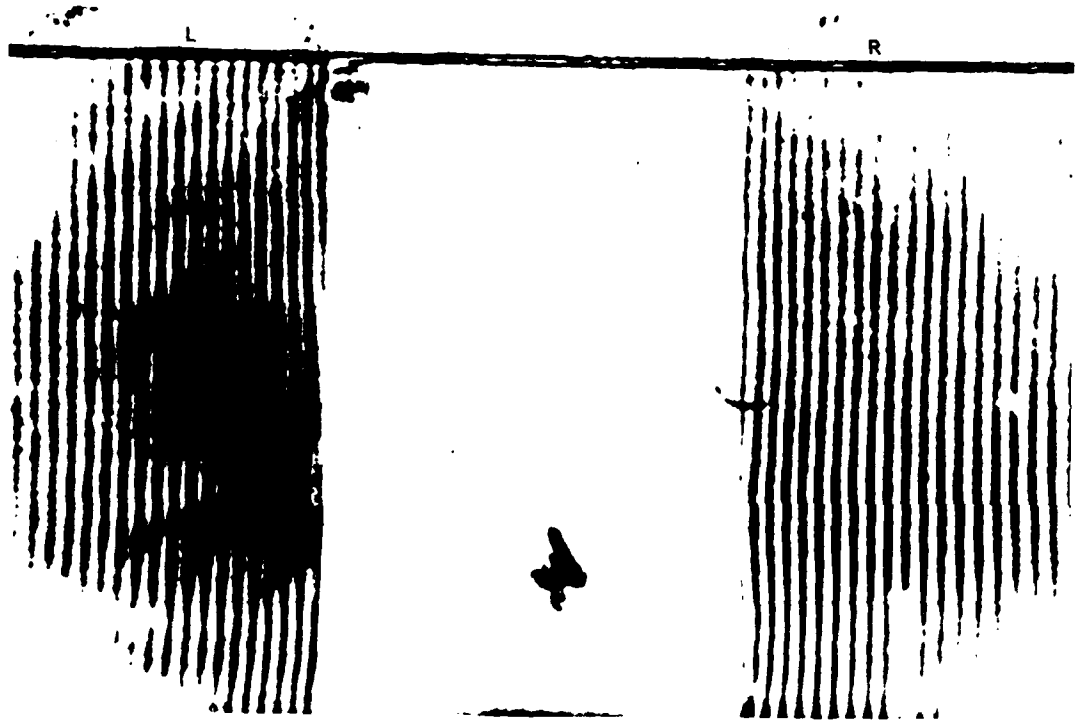

Figure 21. Photograph of Moiré Fringe Pattern with 4th-Step Load on Test Specimen of Mixed Polyester 60:40.

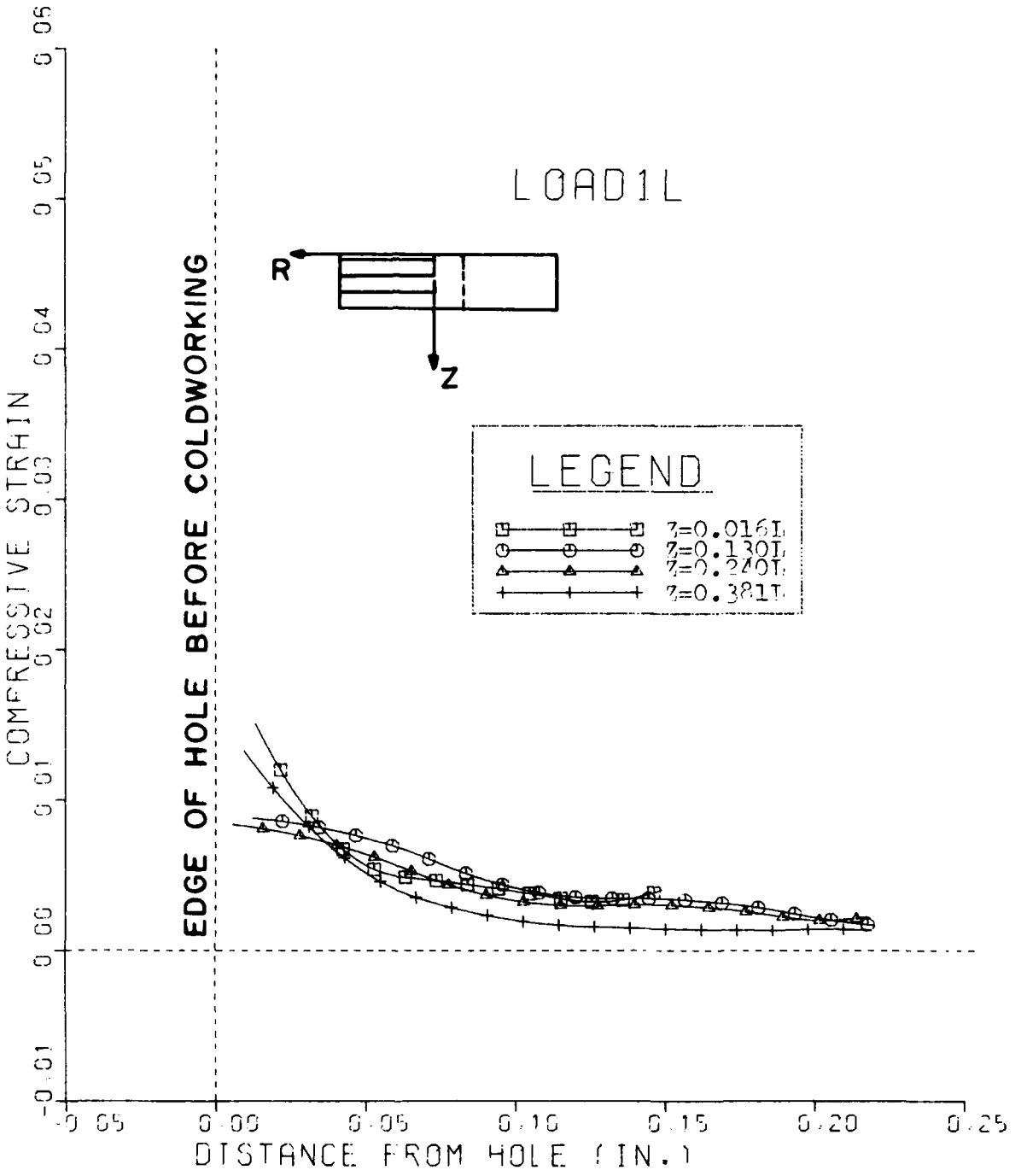

Figure 22. Radial Strain at Different Planes Along the Thickness on Left Side of Hole at 1st Step.

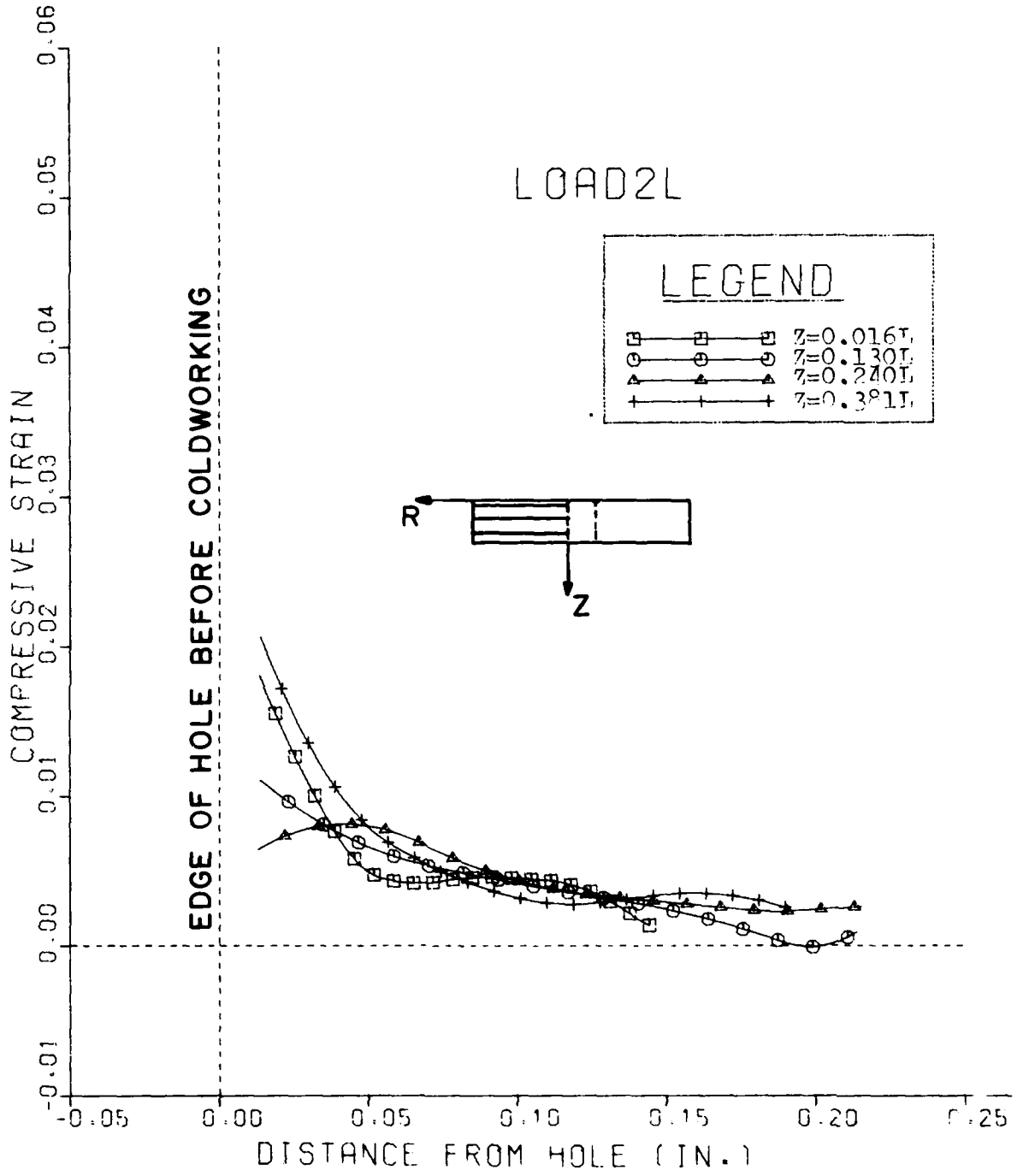

Figure 23. Radial Strain at Different Planes Along the Thickness on Left Side of Hole at 2nd Step.

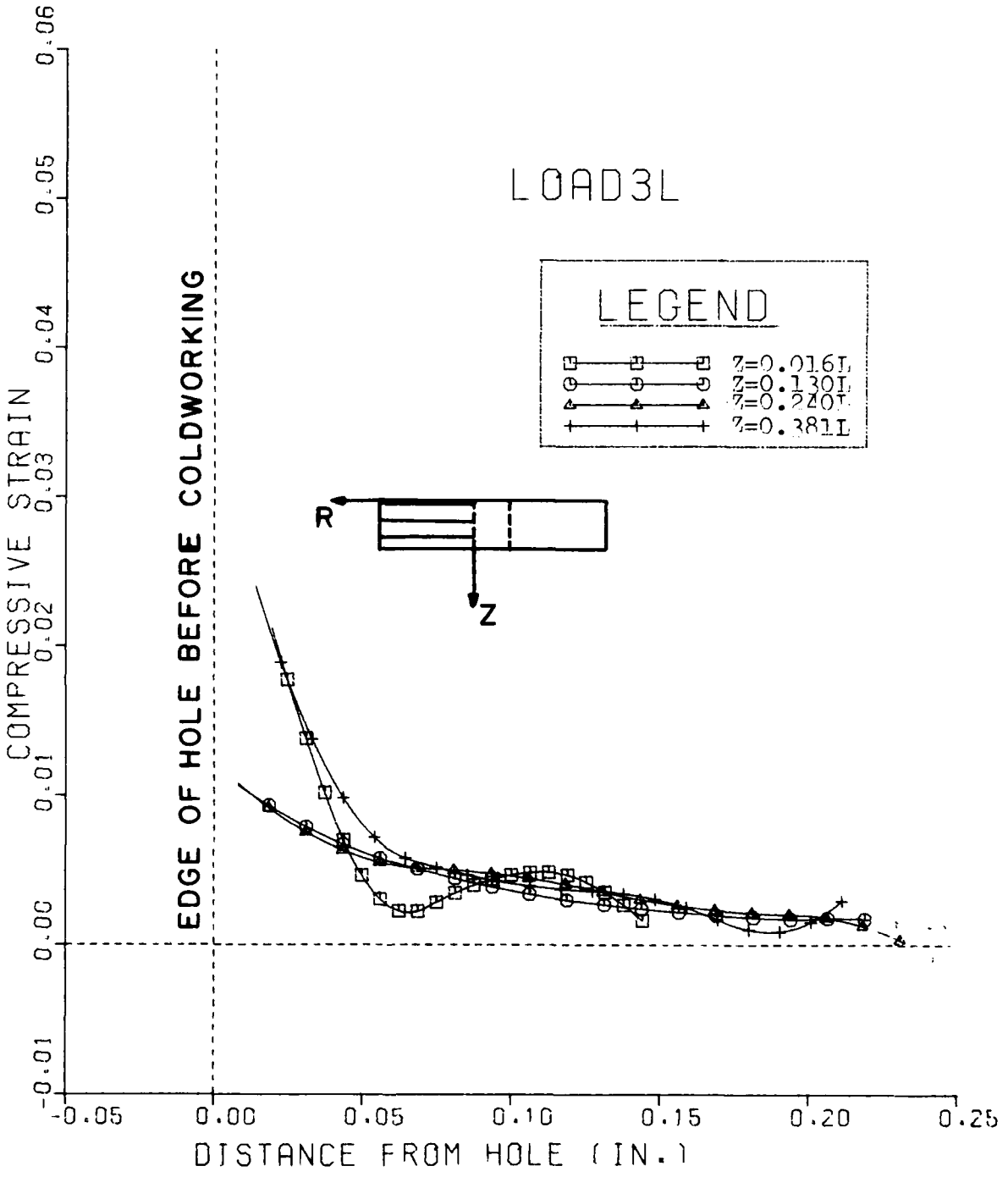

Figure 24. Radial Strain at Different Planes Along the Thickness on Left Side of Hole at 3rd Step.

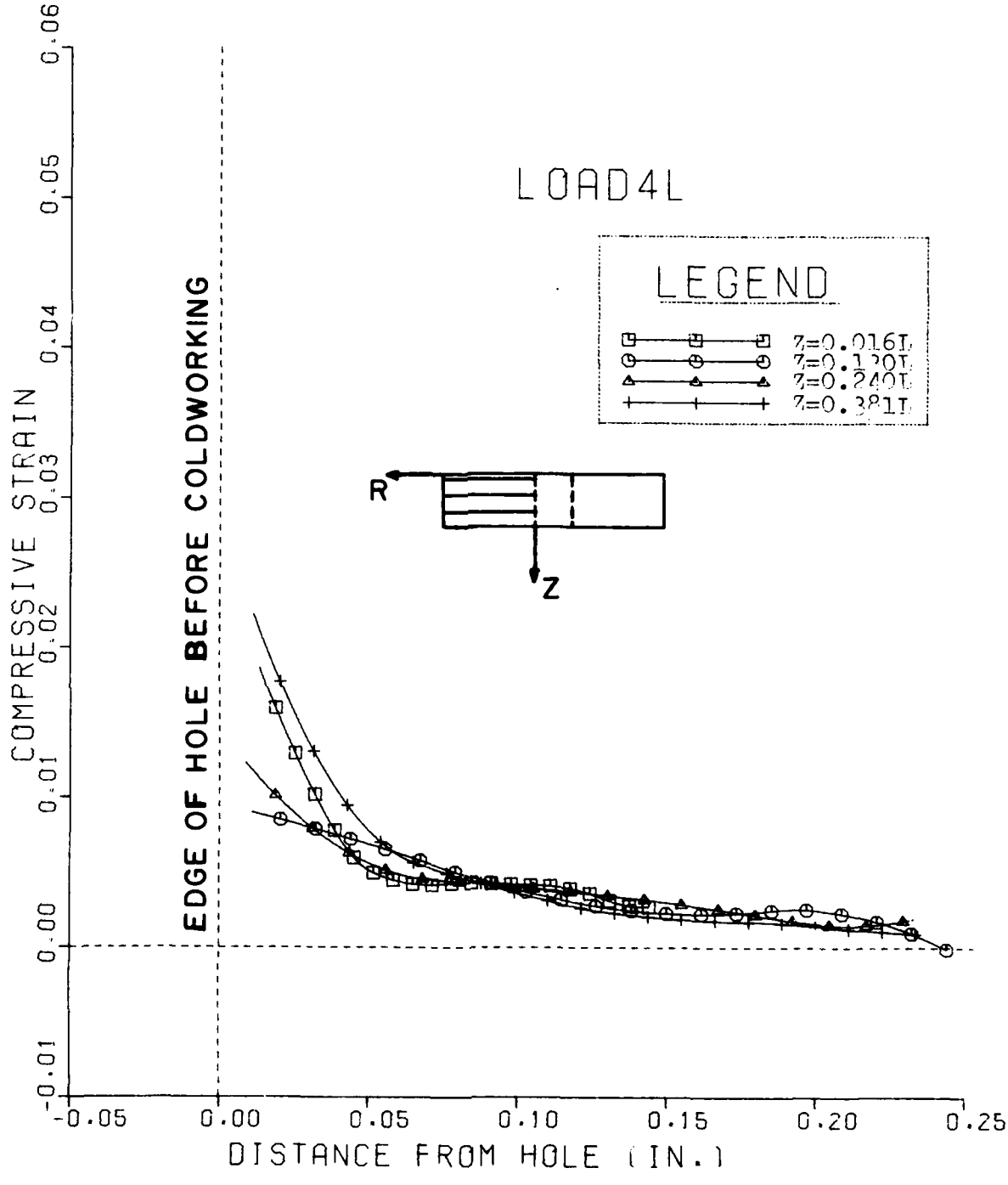

Figure 25. Radial Strain at Different Planes Along the Thickness on Left Side of Hole at 4th Step.

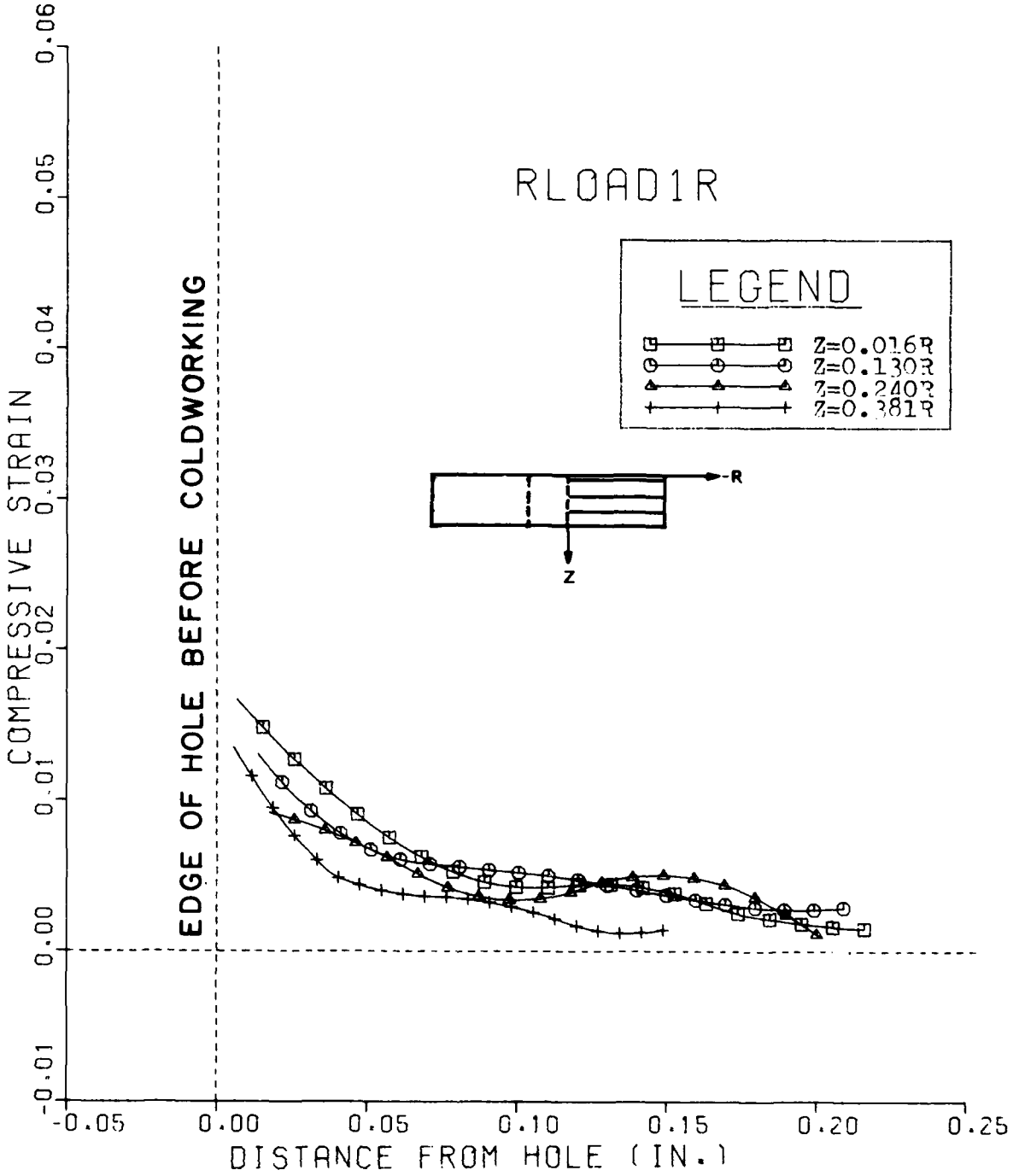

Figure 26. Radial Strain at Different Planes Along the Thickness on Right Side of Hole at 1st Step.

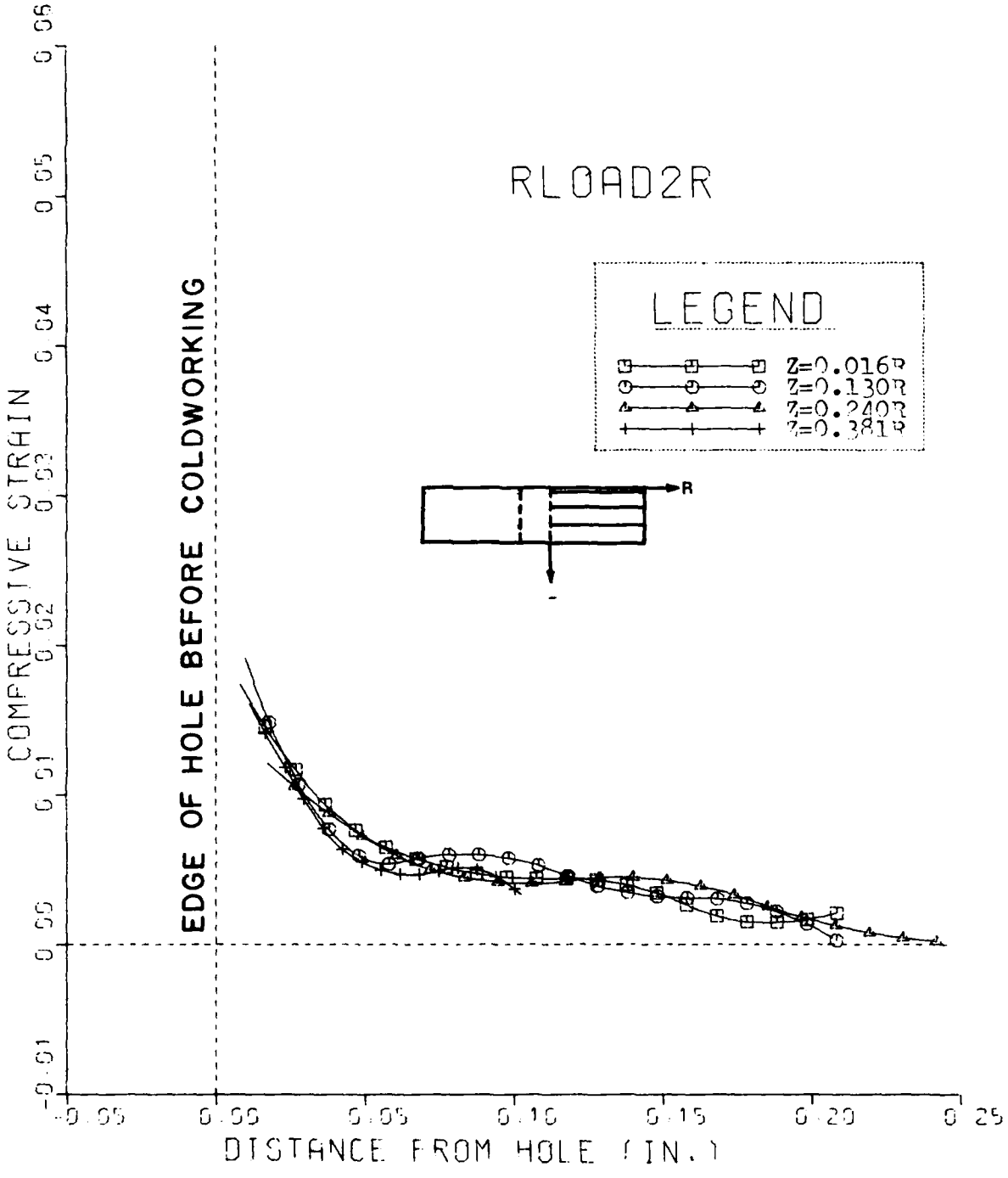

Figure 27. Radial Strain at Different Planes Along the Thickness on Right Side of Hole at 2nd Step.

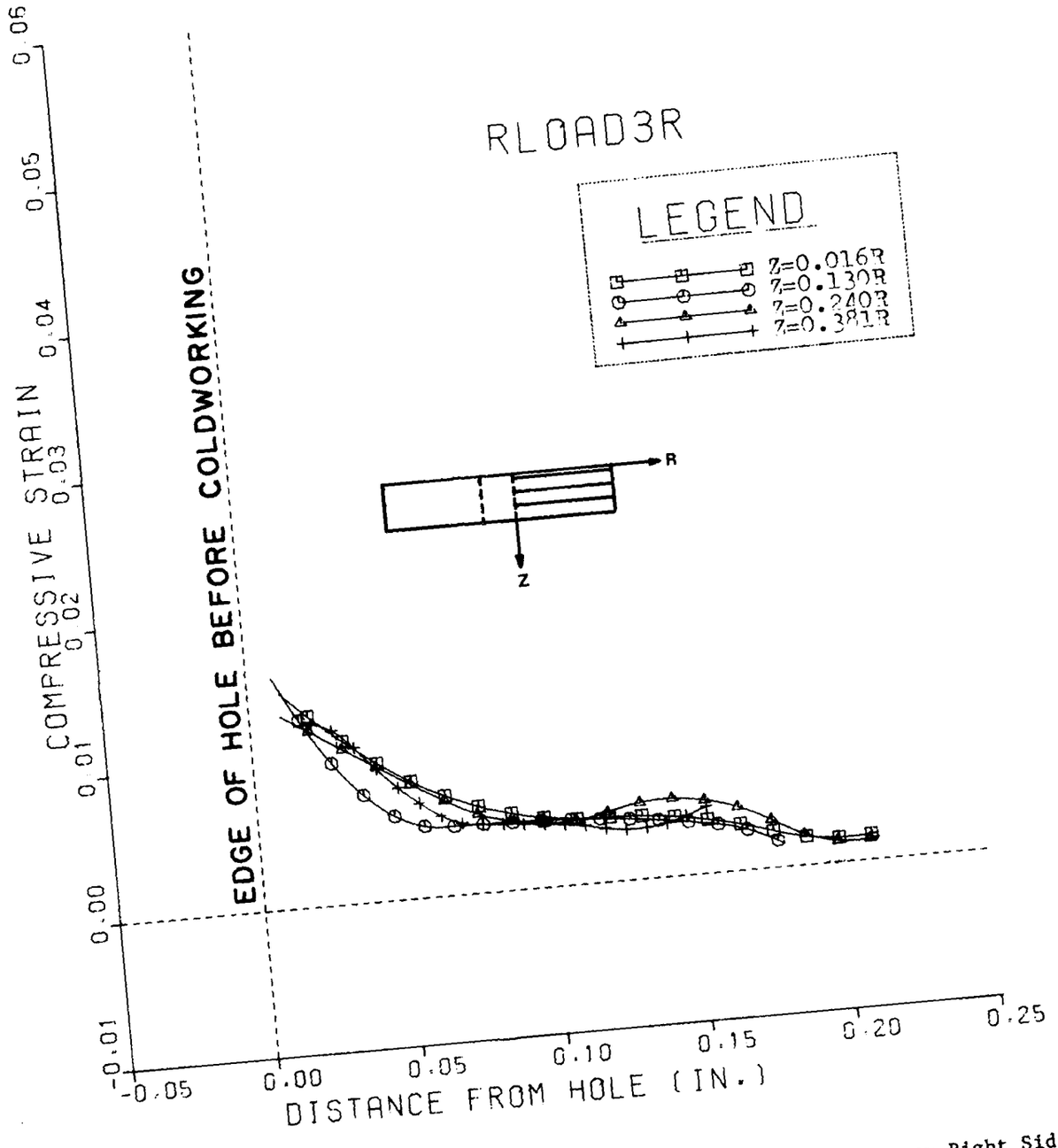

Figure 28. Radial Strain at Different Planes Along the Thickness on Right Side of Hole at 3rd Step.

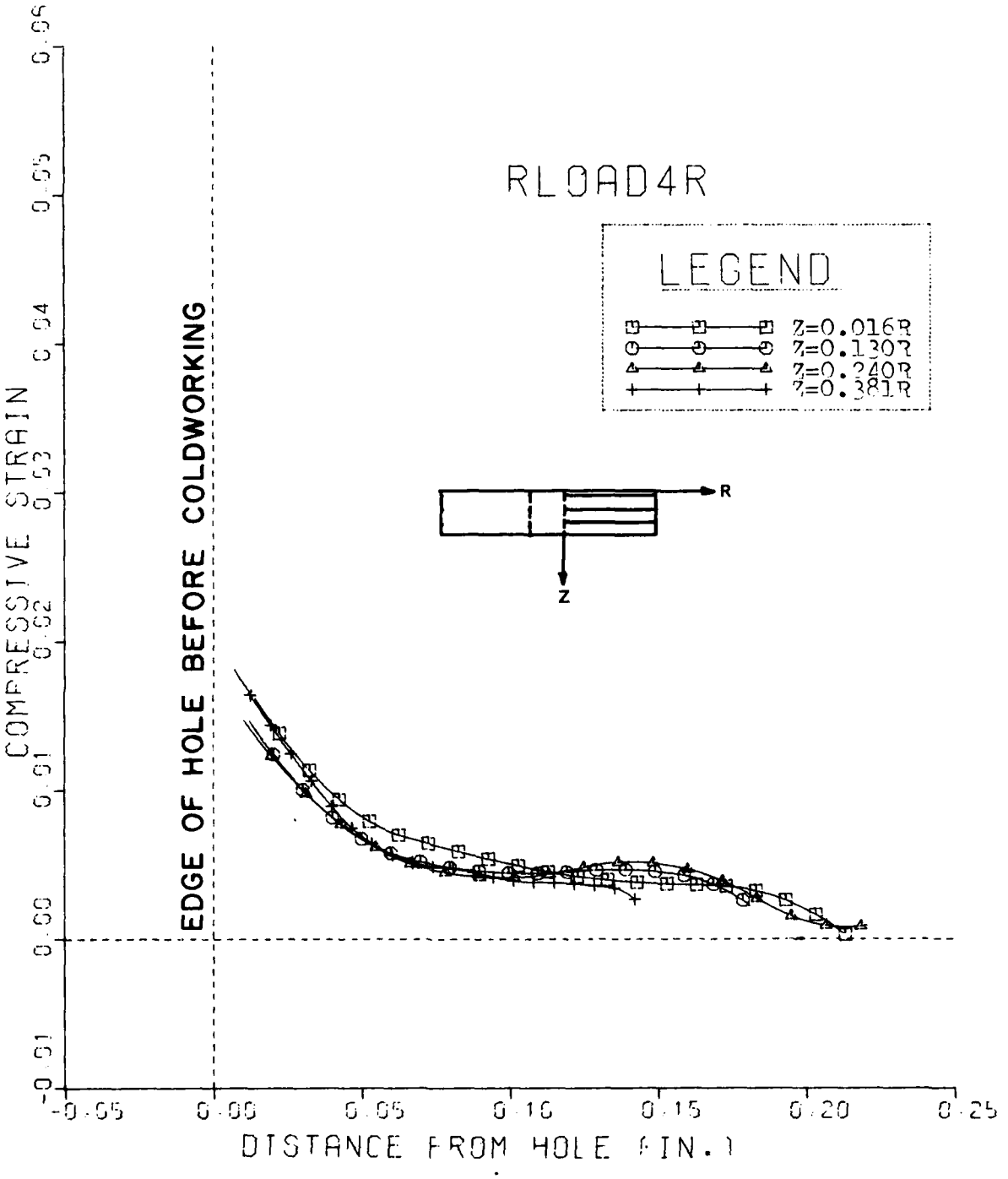

Figure 29. Radial Strain at Different Planes Along the Thickness on Right Side of Hole at 4th Step.

after the mandrel was pulled out. The strain is maximum at the top and decreases towards the bottom as shown in Figure 22 and Figure 26. The shape of the fringe line pattern obviously changes as the mandrel is pulled through. From Figures 19 and 20, we can see a modification of the fringe pattern near the top of the mandrel when the mandrel was pulled down for each step (the position of the top of the mandrel is shown by the arrow). When the tapered mandrel was pulled out, the strain on the bottom surface was slightly larger than at the top, and the strains inside the specimen were smaller than the surface strains, as shown in Figures 25 and 29, because the diametral expansion was smaller than on the surface.

The strain in the z-direction for the polyester specimen was measured from moiré fringe patterns to within 0.05 inches (0.13 mm) of the edge of the hole after the tapered mandrel was pulled through and the sleeve was still in the hole. The photographs of the moiré fringe pattern from the horizontal grill (horizontal fringes) are shown in Figure 30 to Figure 34; and the plots of the strain in the z-direction on the left side and the right side of the hole are shown in Figure 35 to Figure 38 and Figure 39 to Figure 42, respectively. The results show that, after the specimen was loaded, the fringe near the edge of the hole moved toward the midplane. The distance between the two fringes in the deformed specimen was smaller than the corresponding distance for the undeformed specimen. At the top of the specimen, the fringes near the edge of the hole moved toward the midplane, but the distance between the two fringes was slightly larger than in the unloaded case. Such behavior occurs because the top layer of the specimen near the edge of the hole is expanded. Unfortunately, the optical system could not record a good enough grating near the bottom surface, and thus, the bottom surface results could not be obtained because of a lack of fringe resolution. The

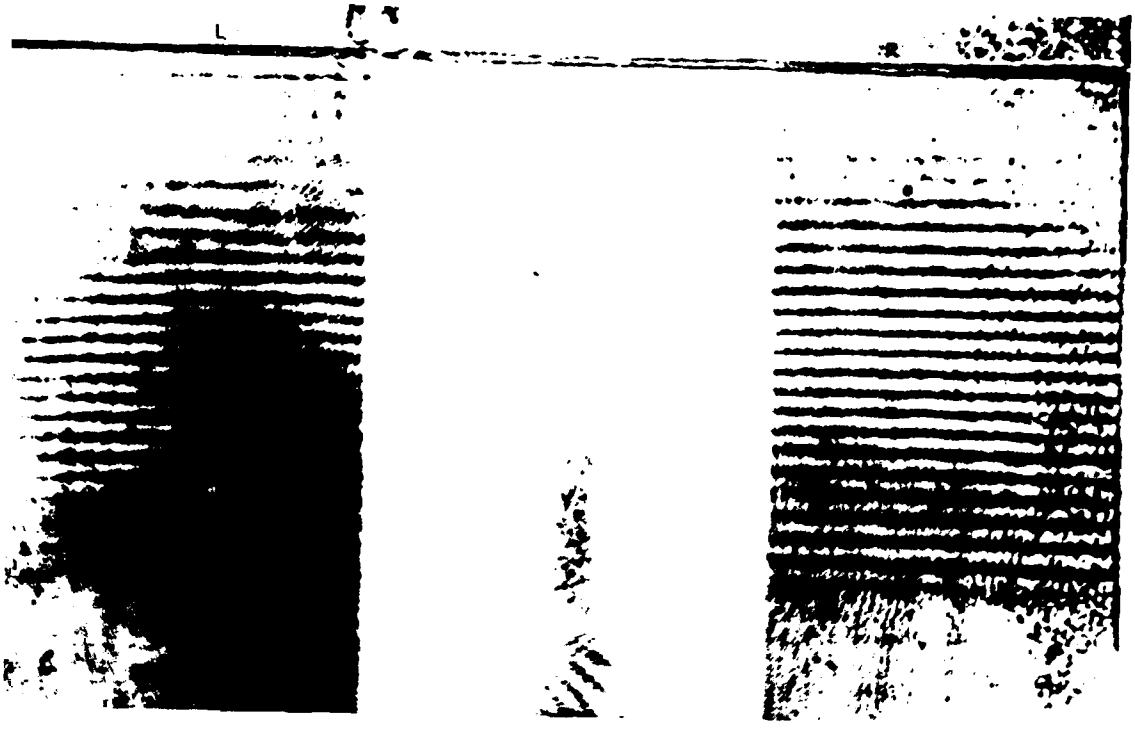

Figure 30 Photograph of Moiré Fringe Pattern with No-Load on Test Specimen of Mixed Polyester 60:40.

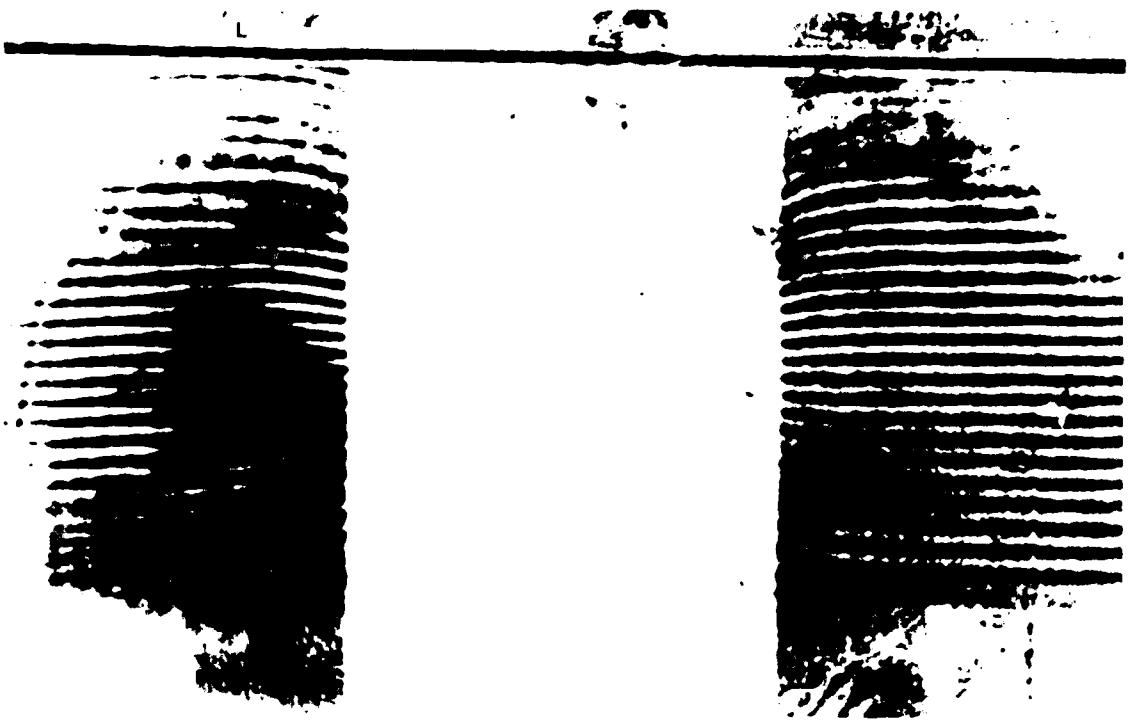

Figure 31. Photograph of Moiré Fringe Pattern with 1st-Step Load on Test Specimen of Mixed Polyester 60:40.

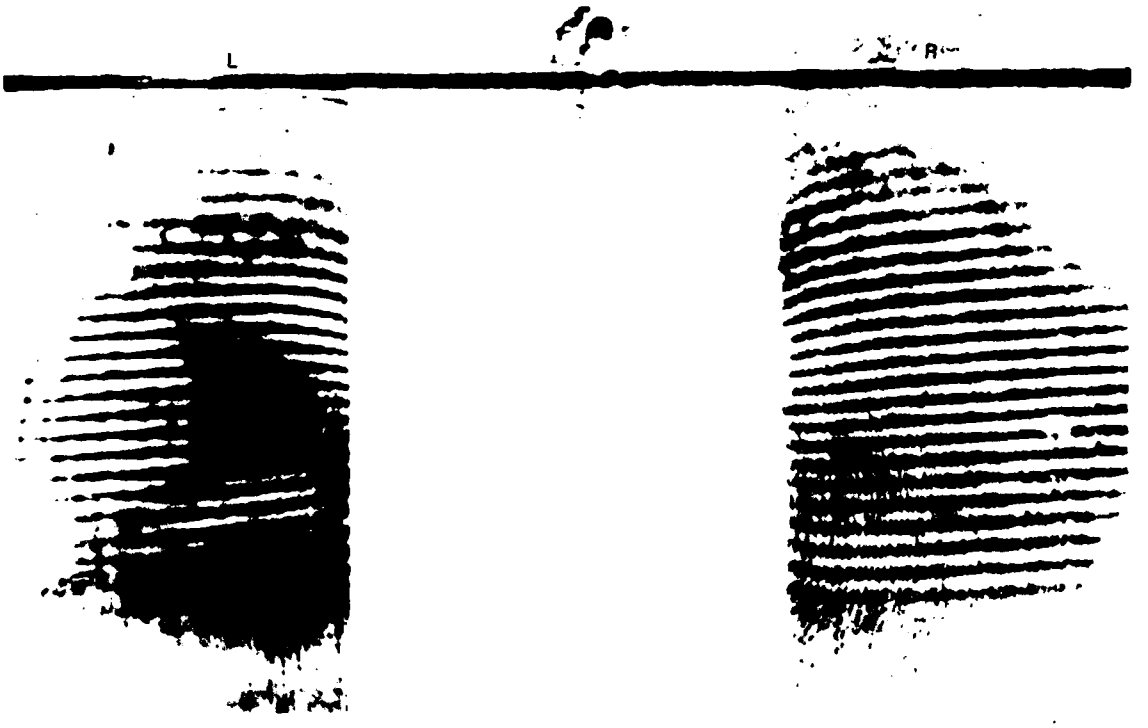

Figure 32. Photograph of Moiré Fringe Pattern with 2nd-Step Load on Test Specimen of Mixed Polyester 60:40.

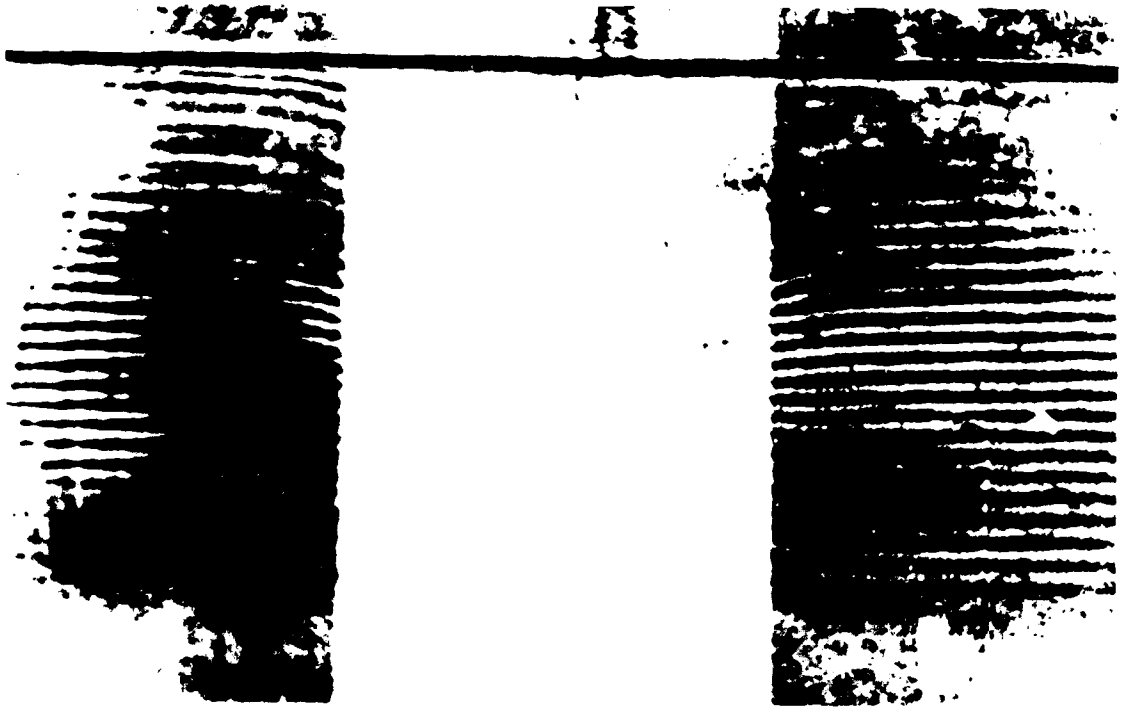

Figure 33. Photograph of Moiré Fringe Pattern with 3rd-Step Load on Test Specimen of Mixed Polyester 60:40.

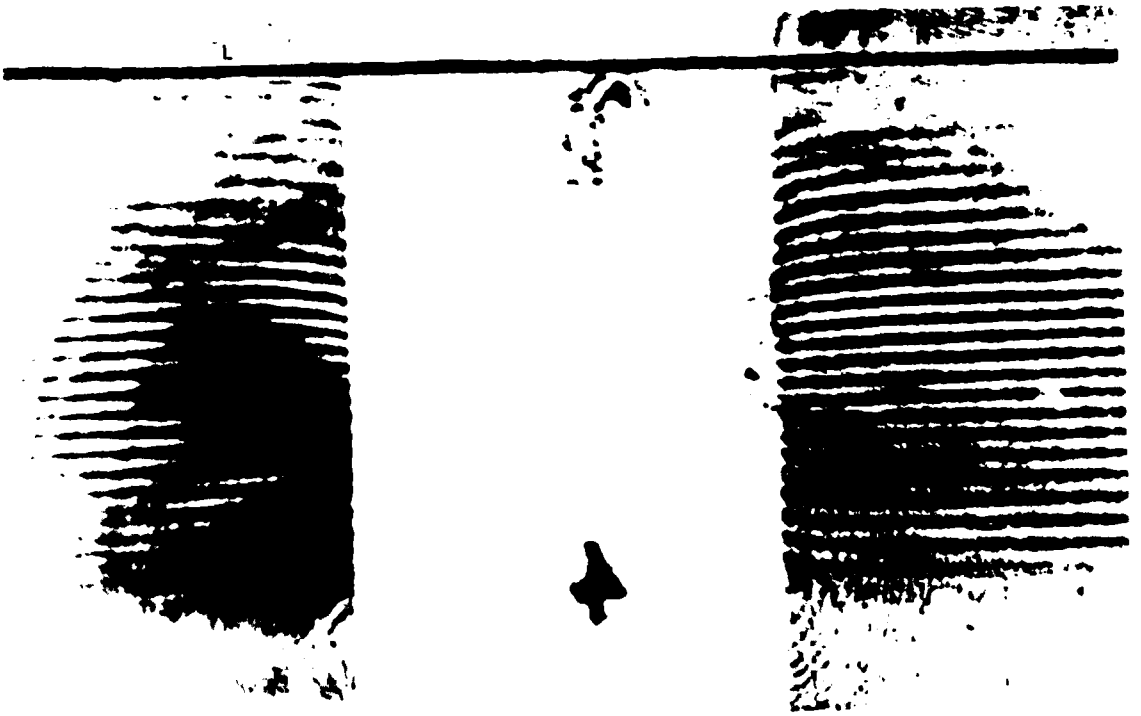

Figure 34. Photograph of Moiré Fringe Pattern with 4th-Step Load on Test Specimen of Mixed Polyester 60:40.

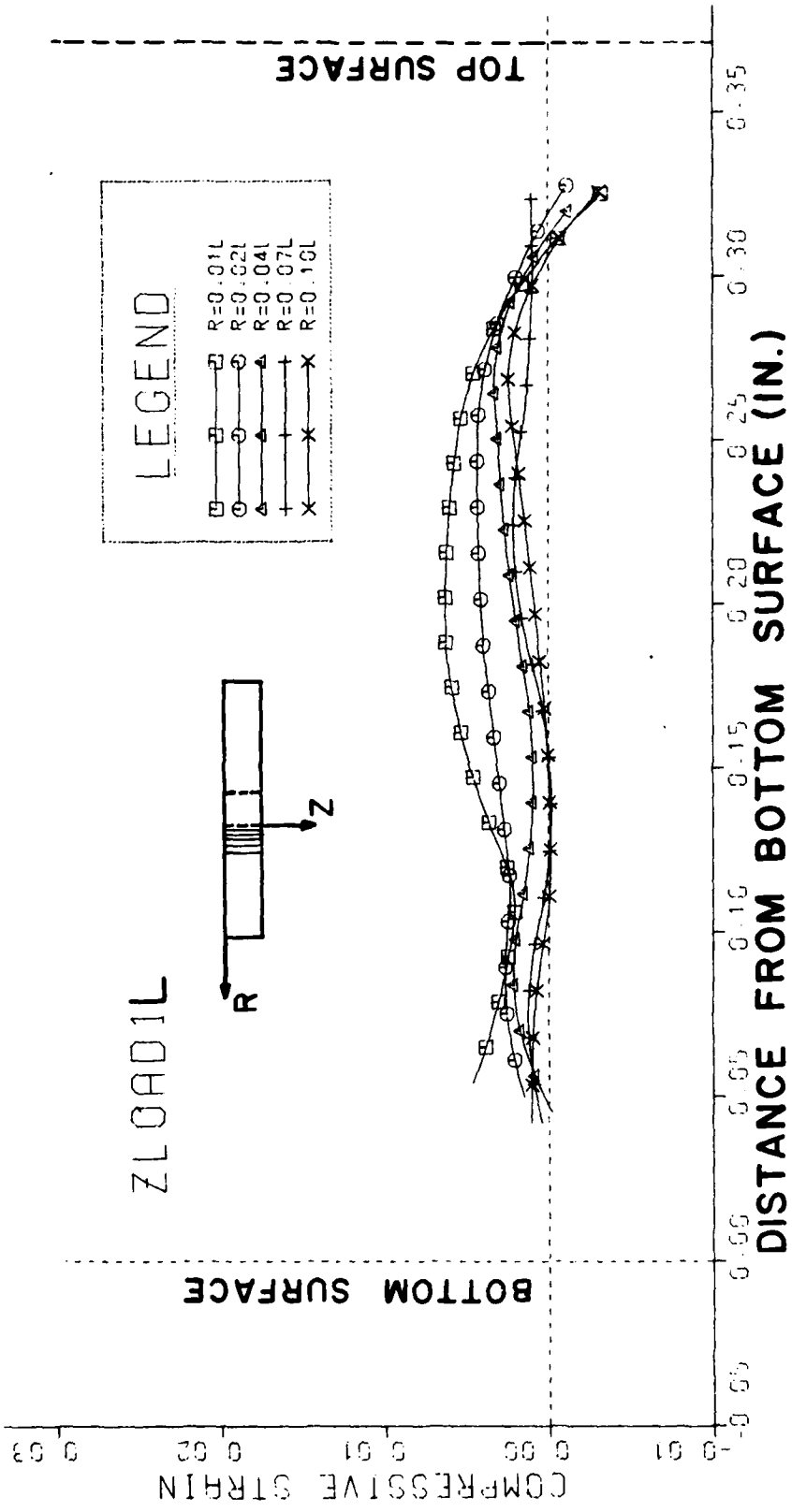

Figure 35. Strain in Z-Direction at Different Lines on Left Side of Hole at 1st Step.

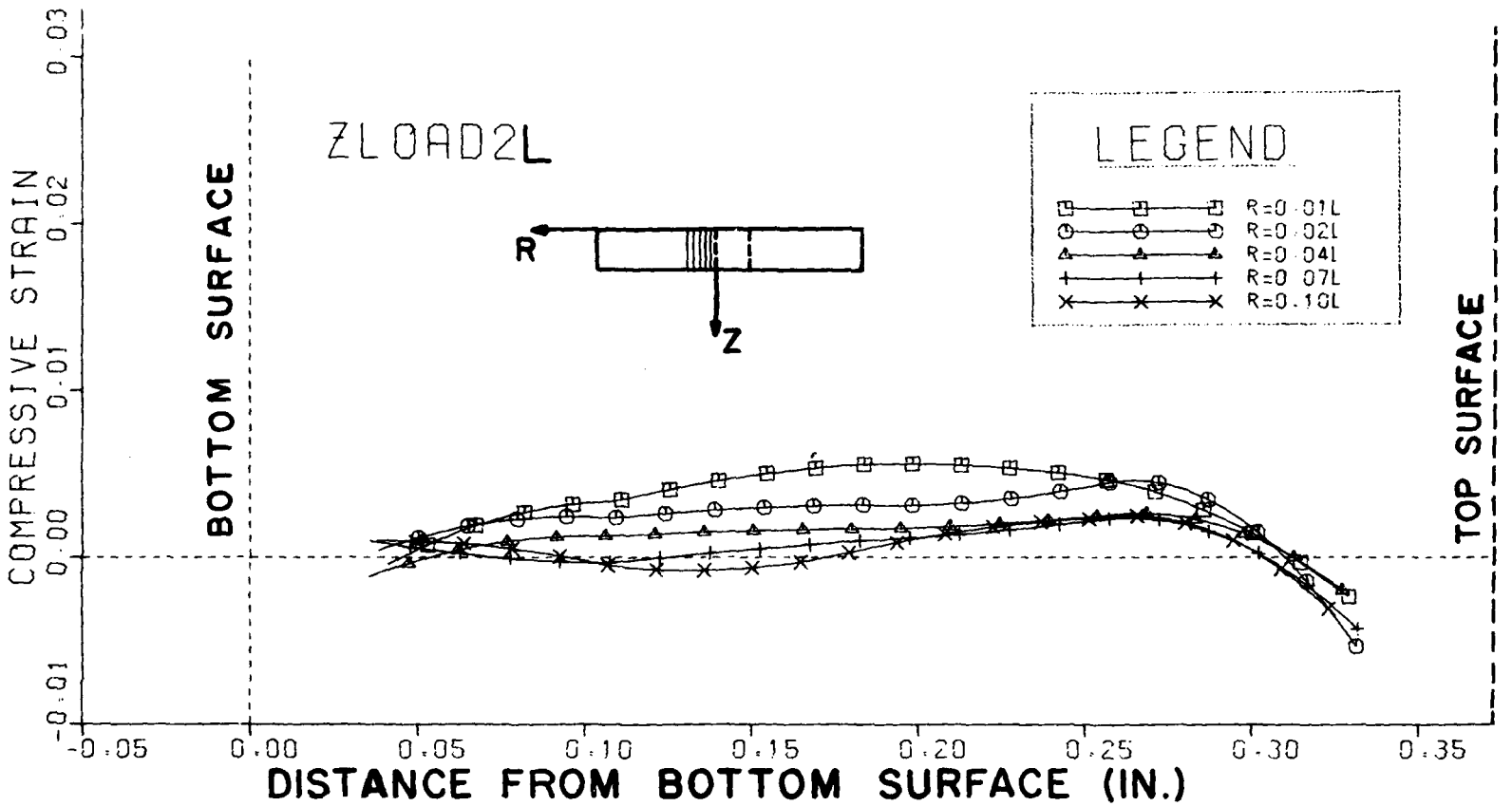

Figure 36. Strain in Z-Direction at Different Lines on Left Side of Hole at 2nd Step.

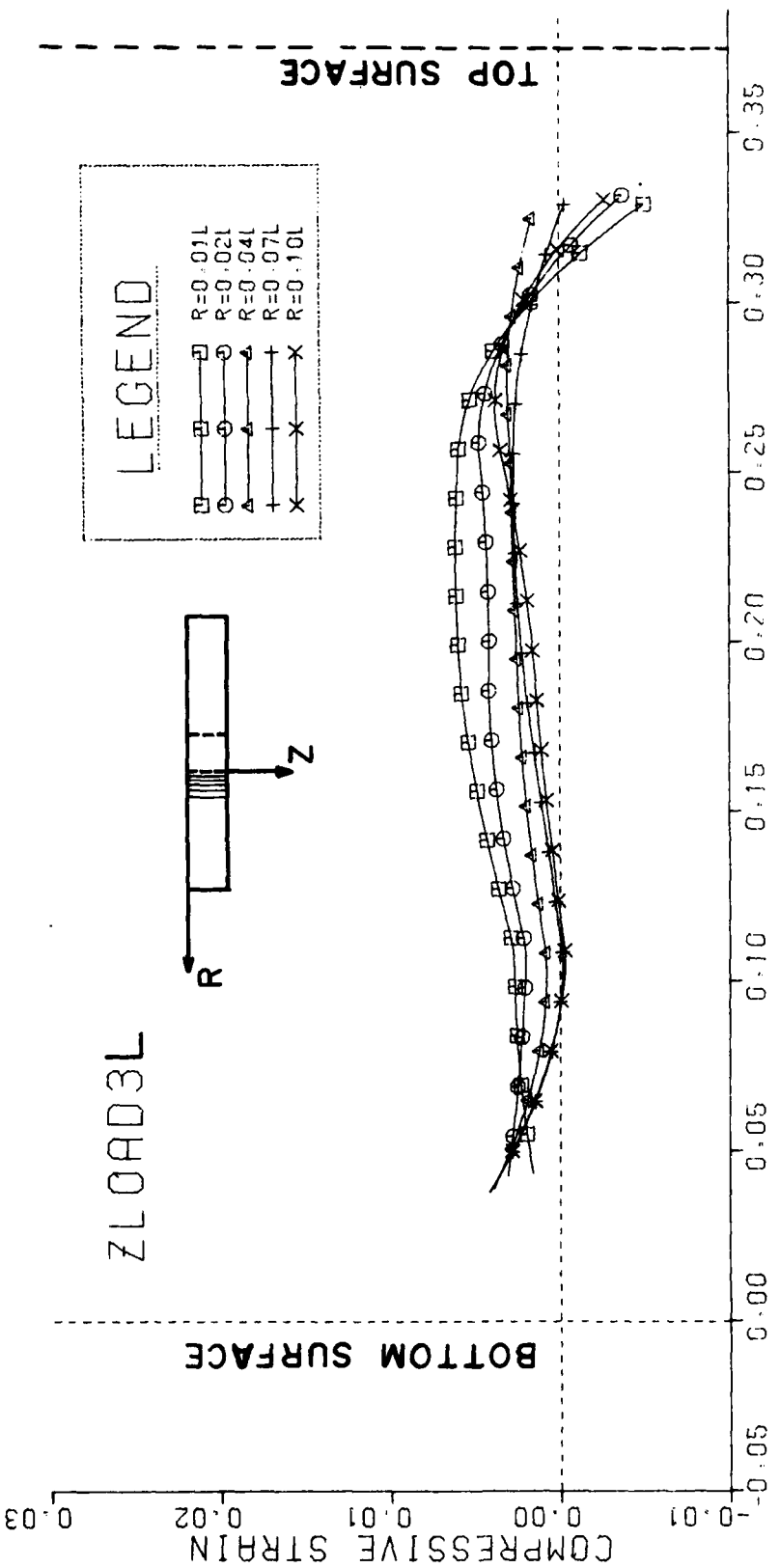

Figure 37. Strain in Z-Direction at Different Lines on Left Side of Hole at 3rd Step.

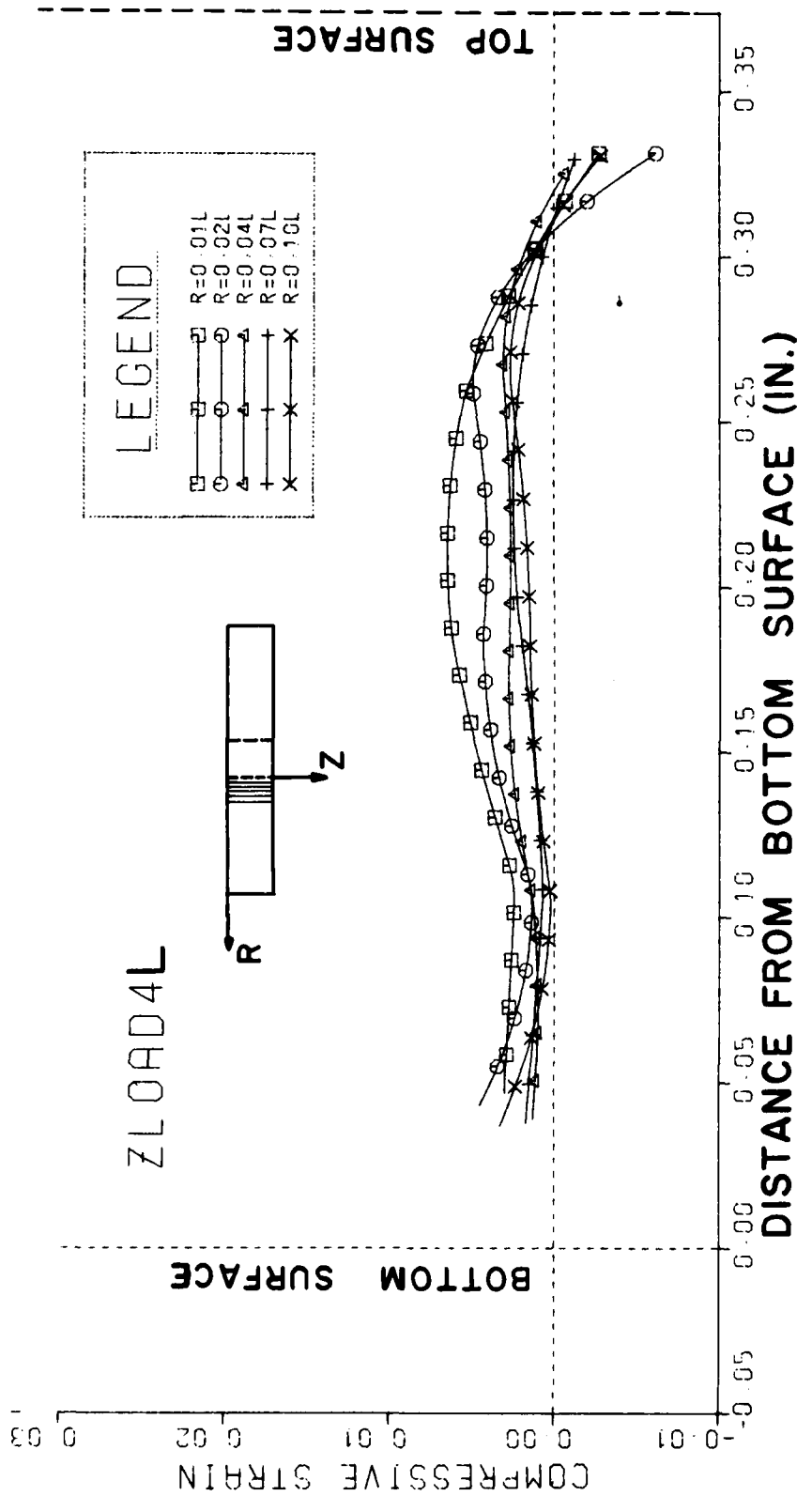

Figure 38. Strain in Z-Direction at Different Lines on Left Side of Hole at 4th Step.

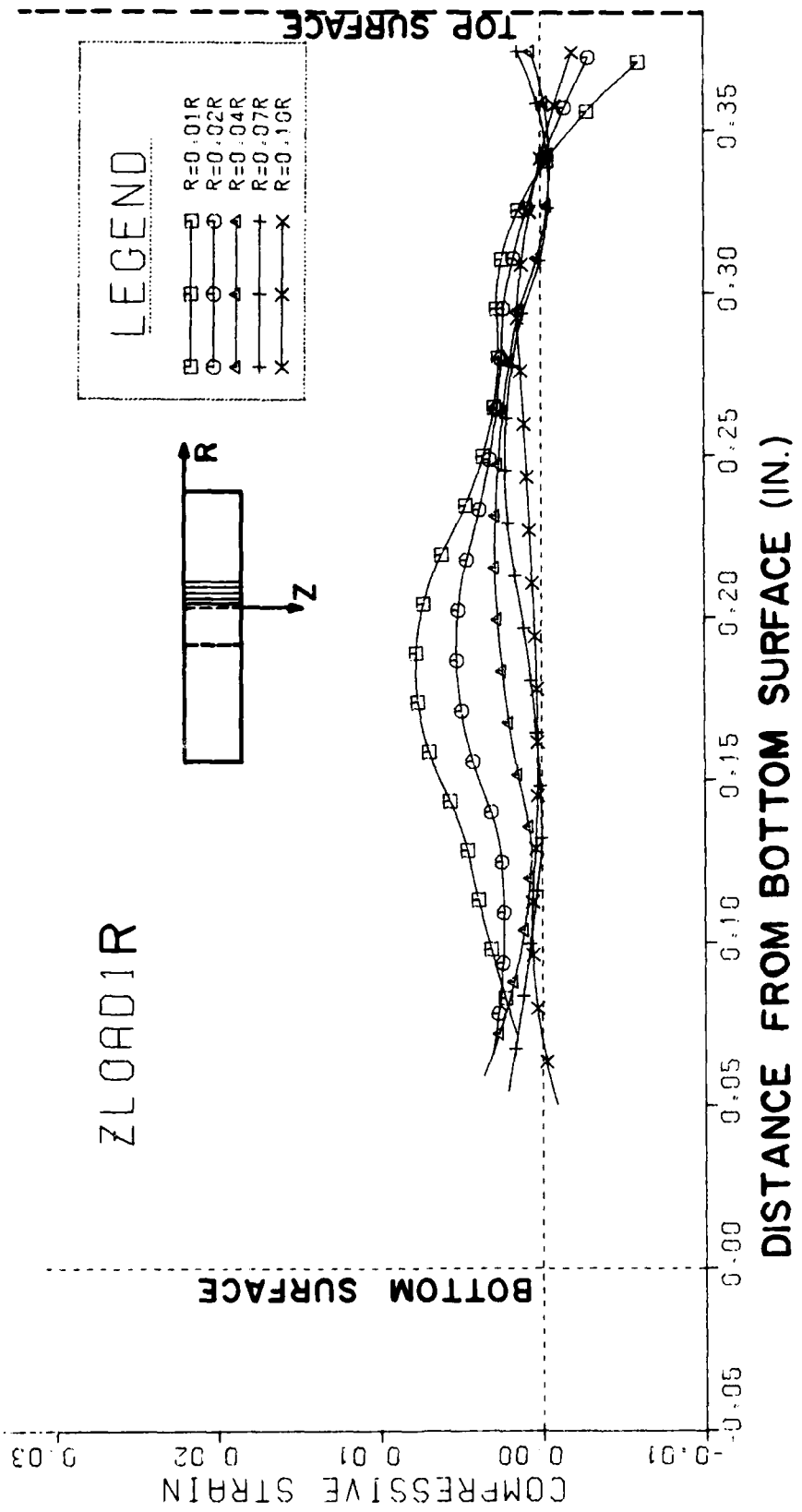

Figure 39. Strain in Z-Direction at Different Lines on Right Side of Hole at 1st Step.

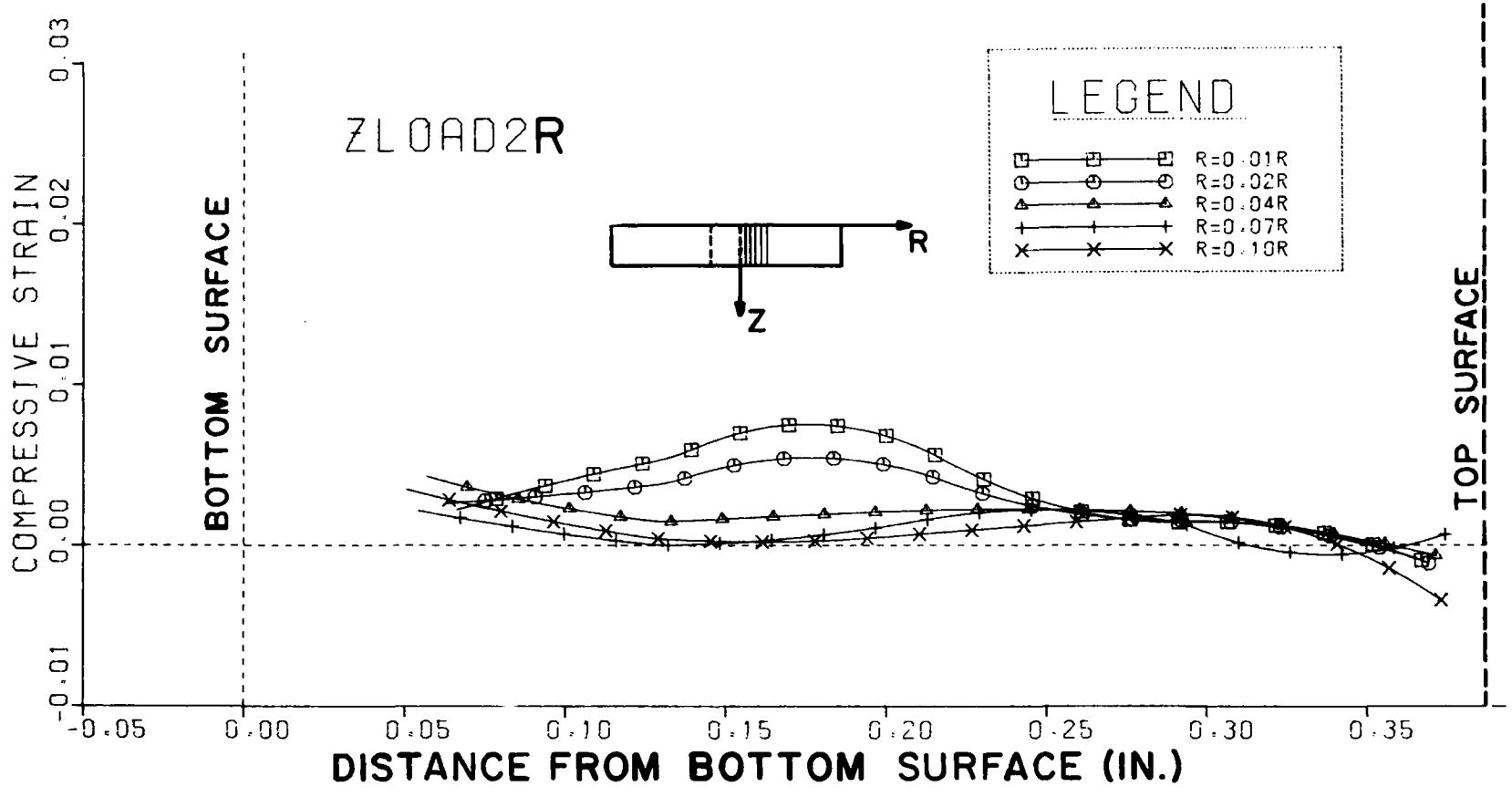

Figure 40. Strain in Z-Direction at Different Lines on Right Side of Hole at 2nd Step.

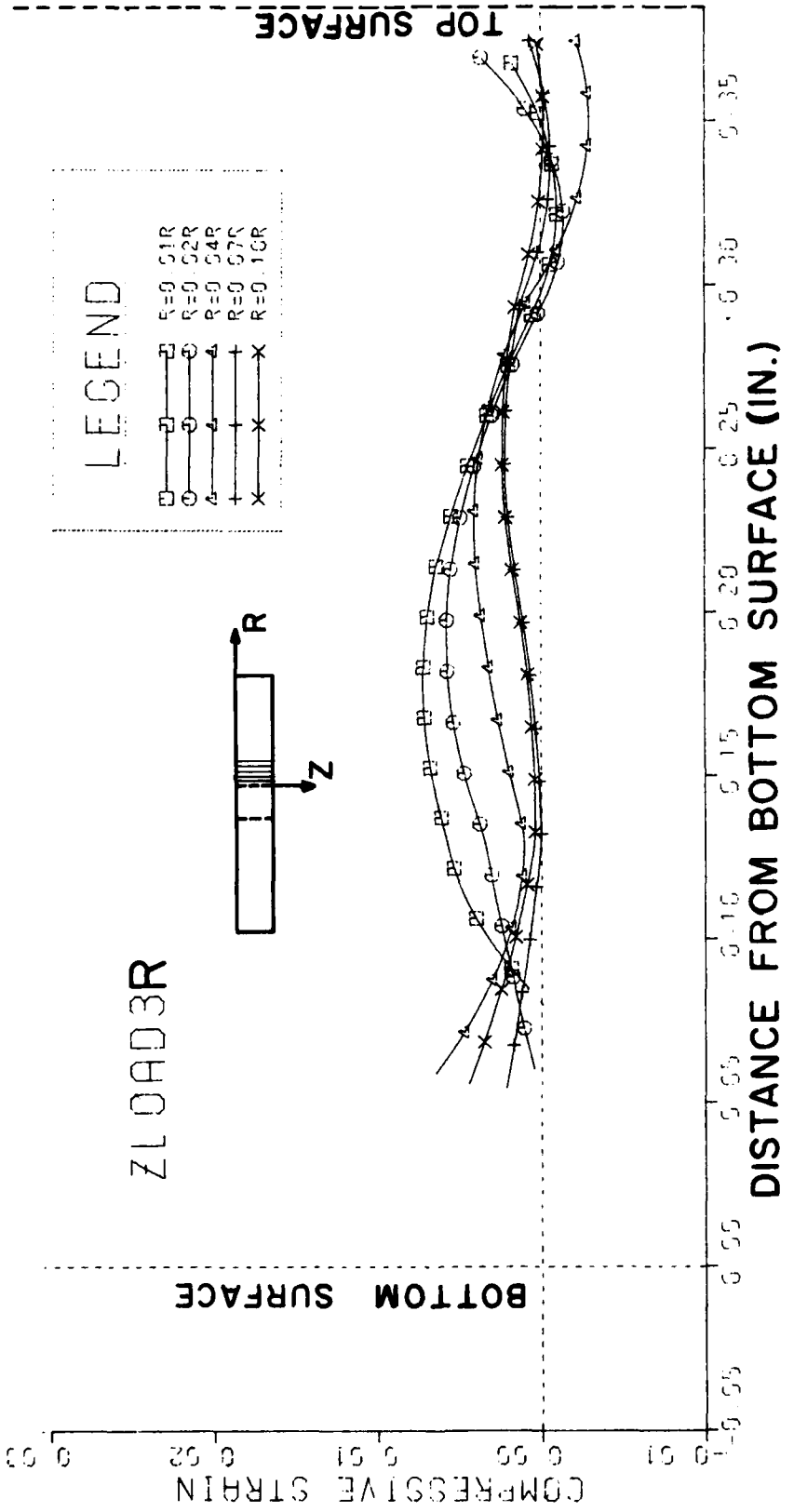

Figure 41. Strain in Z-Direction at Different Lines on Right Side of Hole at 3rd Step.

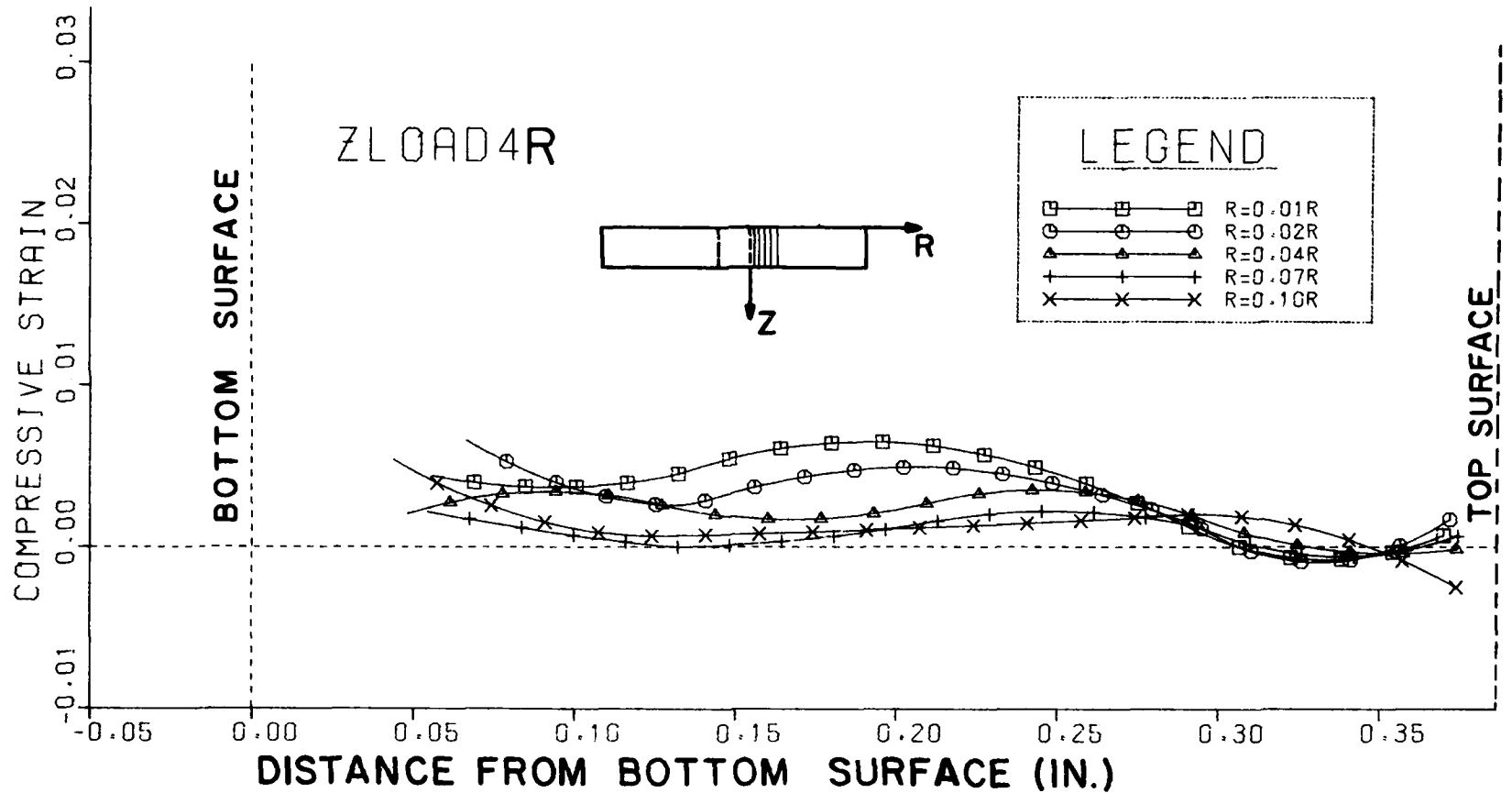

Figure 42. Strain in Z-Direction at Different Lines on Right Side of Hole at 4th Step.

strain near the edge of the hole along the z-direction is tension near the top surface, but it changes to a compressive strain farther than a few millimeters from the surface. The strain increases to a maximum compressive strain at about the midplane, decreases to near zero and then increases to compression again as the bottom surface is approached. These changes in sign result from the physical constraints of the process. When the tapered mandrel is pulled down, the bottom surface is supported by an anvil, and the area near the edge of the hole on the bottom surface cannot move down. This constraint causes increasing compressive strain near the bottom surface.

The strain in the z-direction along the thickness is compression because the taper shape of the mandrel causes a compressive force in the z-direction when the mandrel is pulled down. The maximum strain occurred at about the midplane of the thickness. The vertical displacement near the edge of the hole results in a tension strain for only a thin layer near the top surface. This result agrees with the experimental measurement of the thickness change near the edge of the hole on the top surface of a coldwork specimen by S. Poolsuk and W. N. Sharpe, Jr. (11) They showed that the thickness near the edge of the hole on the top surface was expanded after coldwork.

A plot of the strain in the z-direction verses distance from the edge of the hole on the midplane of the fully coldworked specimen is shown in Figure 43. The strain is maximum near the edge of the hole and then decreases with increasing distance from the hole.

The tangential strain, or "hoop" strain, can be measured by using a unique multi-plane specimen having embedded gratings. For this study, polycarbonate was used to make a specimen. The specimen was made in a

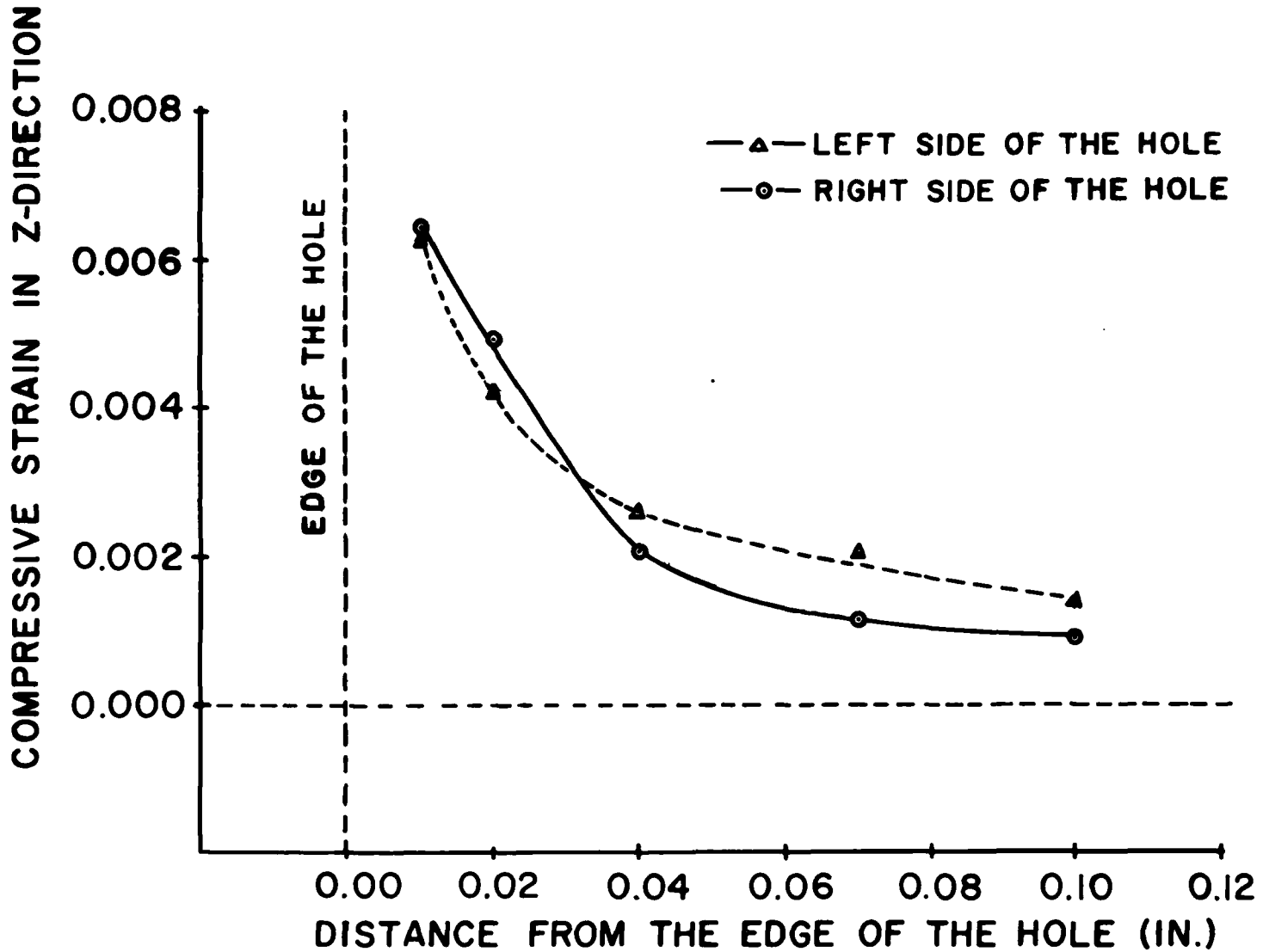

Figure 43. Strain in Z-Direction on the Midplane.

circular disk shape. It consisted of 3 pieces having different thicknesses. Two of the disks had half the thickness of the third. The dimensions of the specimen are shown in Figure 44. A copper grating was deposited on one side of each of the thinner pieces by using the stencil method, then, all three pieces were fastened together with epoxy (Epon 828 and Diethylene triamine 100:8 by weight) by bonding a grating side to a plain side. The resulting composite specimen had a copper grating on the quarter plane and on the midplane. A hole with a diameter of 0.25 inches (6.35 mm) was made at the center of the specimen. Finally a copper grating was deposited on the top surface of the thinner piece. No grating was needed on the back surface because, when the specimen was coldworked, the anvil would destroy the grating around the hole. Before coldwork, the anvil was removed from the sleeve and the flange that supported the anvil was trimmed to be as small as possible in order to allow the light to pass through the specimen. This was done so that a photograph of the grating on each plane close to the edge of the hole could be made. The diameter of the flange of the sleeve was a little bigger than the diameter of the hole.

The specimen set-up was almost the same as before, the difference being that the specimen was placed on the specimen holder so as to let the light pass through the specimen in the direction parallel to the hole. A photographic process was developed so that each grating could be recorded individually even though it might be obstructed by other gratings. The first data plate was recorded by focusing on the surface grating. Then the specimen was moved closer to the lens to get a focus on the quarter plane and a second data plate was recorded. Finally the specimen was turned around, and after focusing the grating of the midplane, the third data plate was recorded A schematic of the specimen set-up is shown in Figure 45.

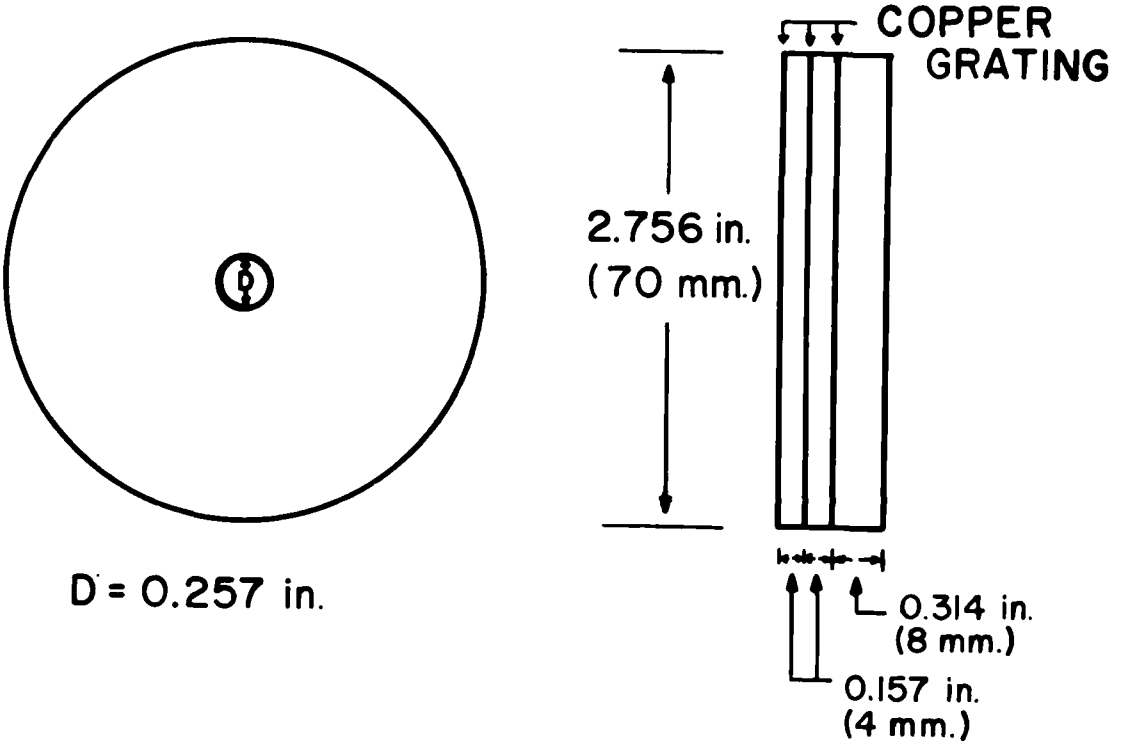

Figure 44. Specimen Dimension.

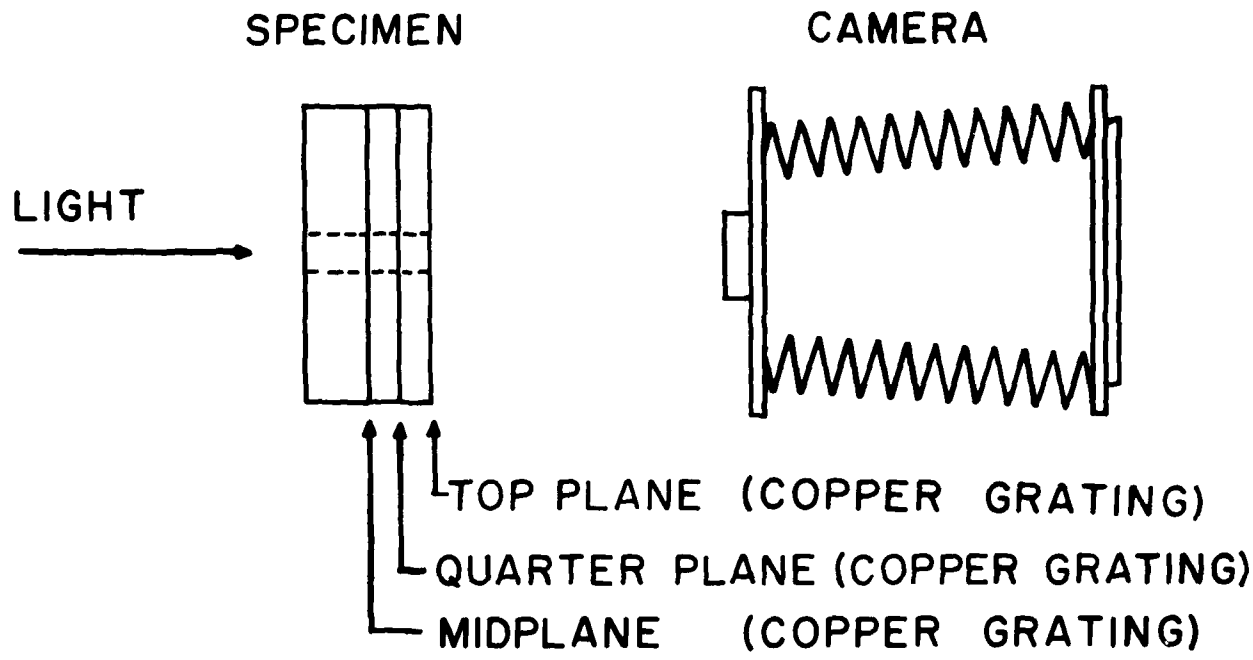

Figure 45. Schematic of the Photographic Data Recording.

For this study, the gratings with no-load and the gratings after mandrelizing were recorded on High Speed Holographic Plate (Kodak Type 131-02, 4x5 inch) for each plane of the grating. The moiré fringe pattern was extracted by using the optical processing technique. The photographs of the moiré fringe pattern on each plane are shown in Figure 46 to Figure 48. The plots of the hoop strains (0.0455 in. from the edge of the hole of the specimen before load) on each plane obtained from the moiré fringe patterns are shown in Figure 49. The results show that the hoop strains near the edge of the hole on each plane are only a little different. The hoop strain on the surface is slightly larger than the others, and the hoop strain on the midplane is the smallest. This agrees with the observation that the diametral expansion on the surface is slightly larger than in the interior of the specimen as was shown in Figure 9.

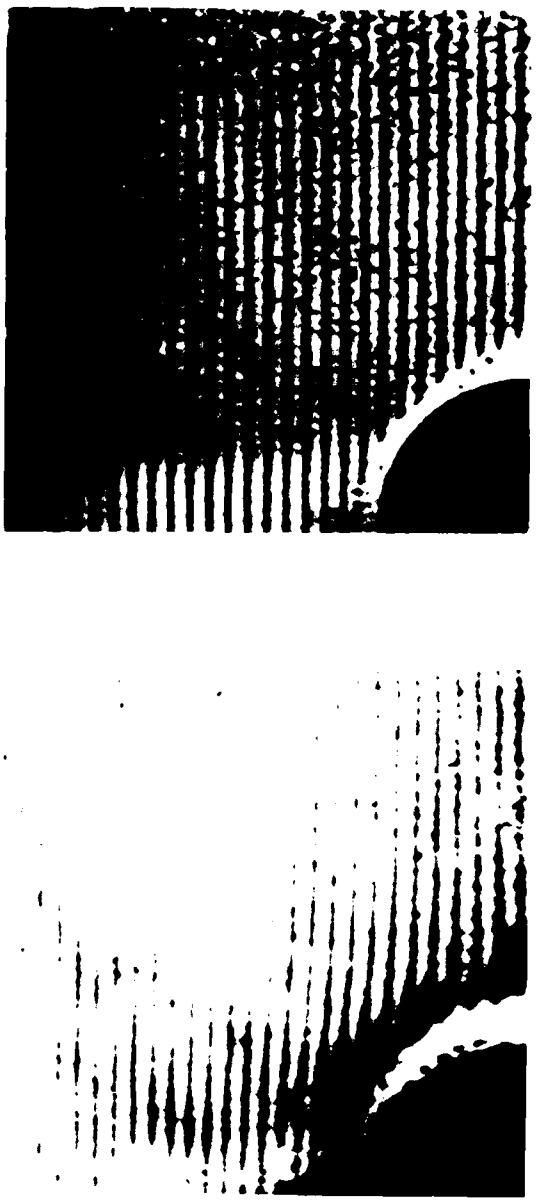

Figure 46. The Moiré Fringe Pattern of Specimen Before and After Load on Surface-Plane.

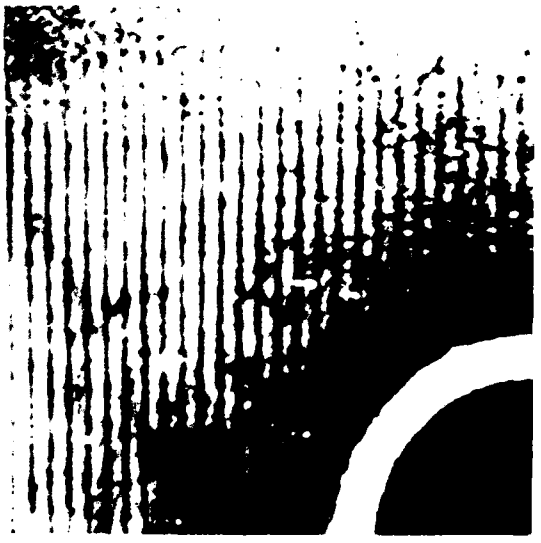

Figure 47. The Moiré Fringe Pattern of Specimen Before and After Load on Quarter-Plane.

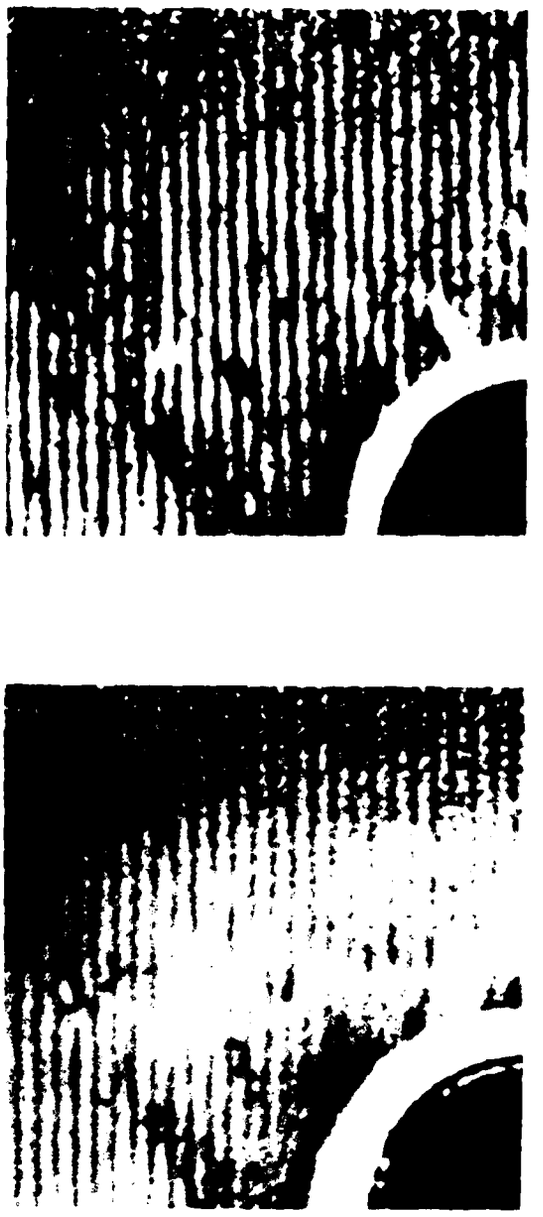

Figure 48. The Moiré Fringe Pattern of Specimen Before and After Load on Mid-Plane.

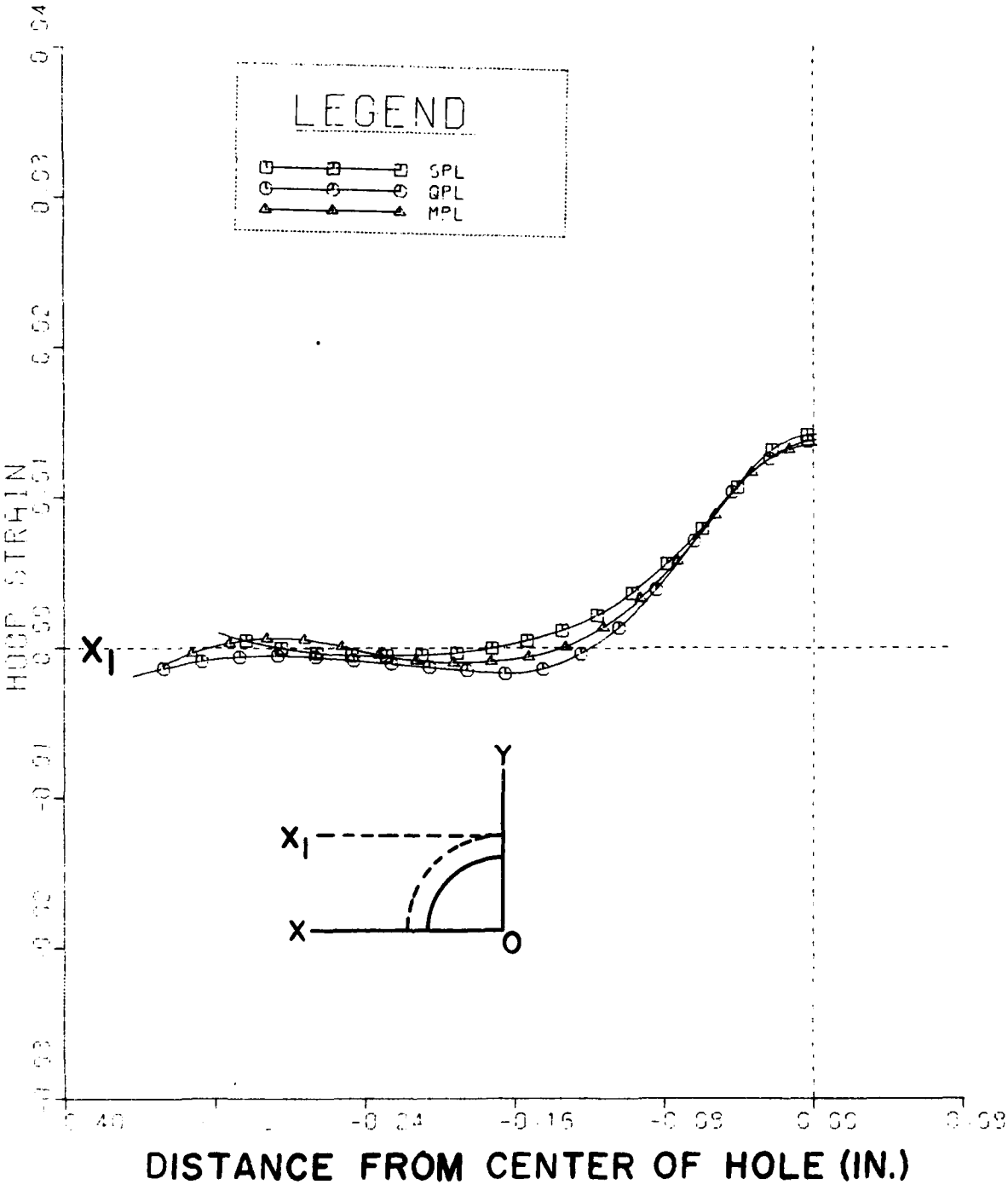

Figure 49. Hoop Strain Near the Edge of the Hole on Different Planes.

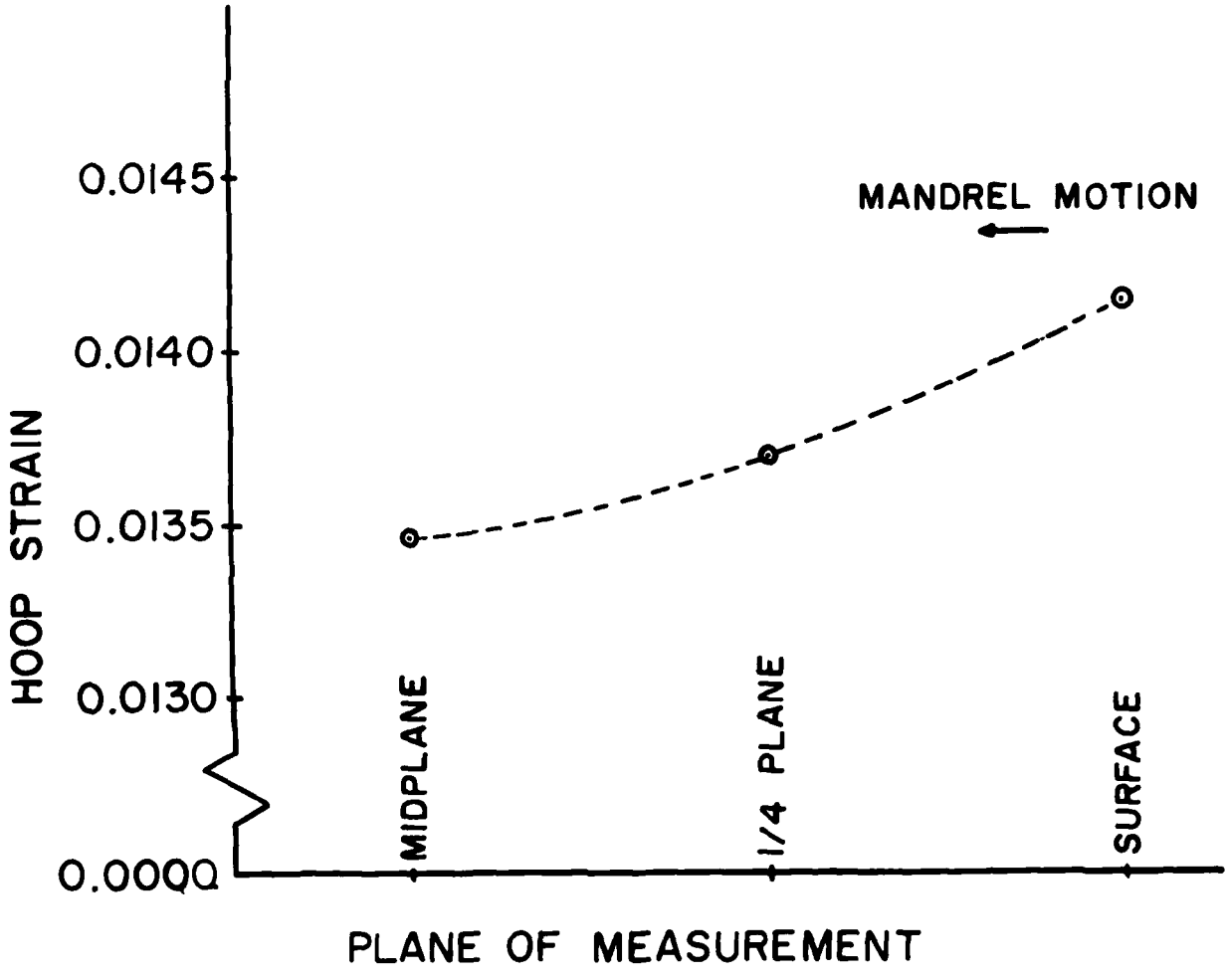

Figure 50. Comparison of Hoop Strain Near the Edge of the Hole on Each Plane.

REFERENCES

1. Residual Surface Strain Distributions Near Holes Which are Coldworked to Various Degrees, by G. L. Cloud, Technical Report AFML-TR-78-153.

2. "Measurement of Strain Fields Near Coldworked Holes," Gary L. Cloud, Experimental Mechanics, 20, 1, 9-16 (January 1980).

3. An Experimental Study of the Interaction of Strain Fields Between Coldworked Fastener Holes, by G. L. Cloud and Mark Tipton, Technical Report AFWAL-TR-80-4205.

4. An Experimental Study of Large Compressive Loads Upon Residual Strain Fields and the Interaction Between Surface Strain Fields Created by Coldworking Fastener Holes, by Gary Cloud and Rajab Sulaimana, Technical Report AFWAL-TR-80-4206.

5. "The Moiré Method Applied to Three-Dimensional Elastic Problem," C. A. Sciammarella and Fu-pen Chiang, Experimental Mechanics, 4, 11, 313-319 (November 1964).

6. An Engineering Handbook on Merlon Polycarbonate, Mobay Chemical Company, Pittsburgh, Pennsylvania.

7. "A Photomechanics Material for Elastoplastic Stress Analysis," D. H. Morris and W. F. Riley, Experimental Mechanics, 12, 10, 448-453 (October 1972).

8. "The Rapid Deposition of Moiré Grids," A. R. Luxmoore and R. Hermann, Experimental Mechanics, 11, 8, 375-377 (August 1971).

9. "The Production of High-Density Moiré Grids," G. S. Holister and A. R. Luxmoore, Experimental Mechanics, 8, 5, 210-216 (May 1968).

10. "The Measurement of Residual Stress by a Moiré Fringe Method," C. A. Walker and J. McKelvie, SPIE Vol. 136, 1st European Congress on Optics Applied to Metrology (1977).

11. "Measurement of the Elastic-Plastic Boundary Around Coldworked Fastener Holes," S. Poolsuk and W. N. Sharpe, Jr., Journal of Applied Mechanics (paper No. 78-WA/APM 2).

*U.S.Government Printing Office: 1982 — 559-006/5086